Coupling Lattice Boltzmann 3D flow simulation in porous media with X-ray microtomographic imaging

M. Crine

Laboratory of Chemical Engineering
University of Liège, *Belgium*

Liège at the heart of Europe

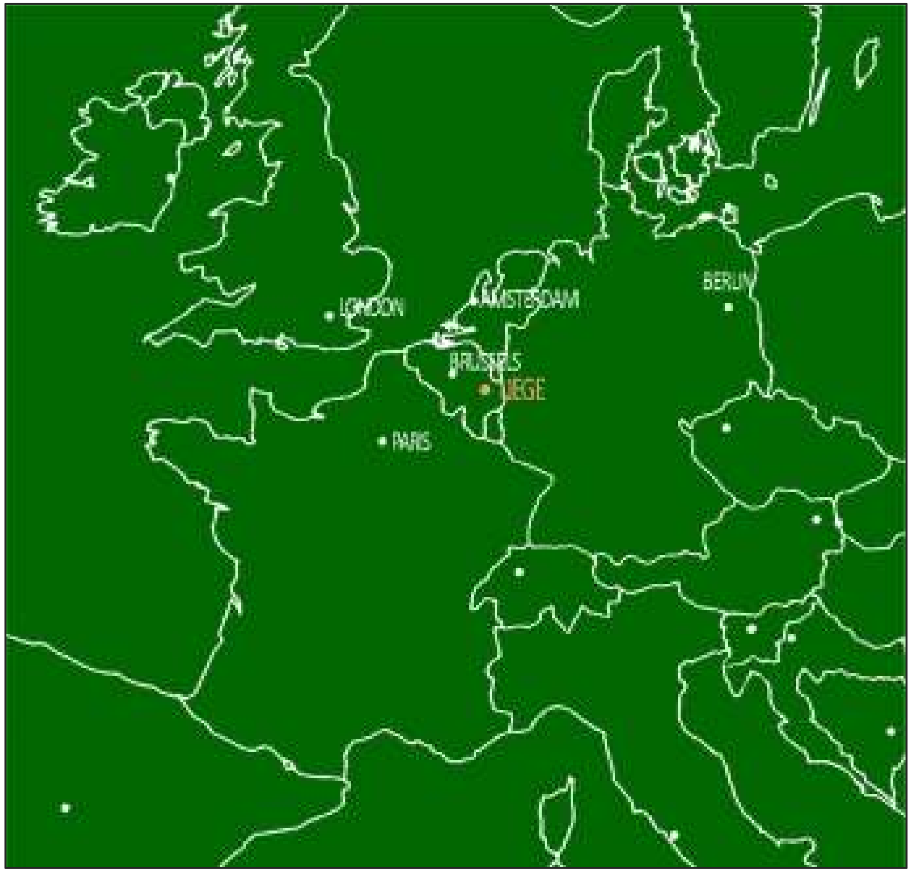

Within 2 European cross-border regions :

- **Meuse-Rhine Euregio**
  - 3 countries (BE, NL, DE)
  - 4 regions
- **University of the Greater Region :**
  - 4 countries (BE, DE, LU, FR)
  - 7 universities
  - 115 000 students
  - 6 000 professors

Université de Liège

LGC CHEMICAL ENGINEERING

Liège: an attracting city

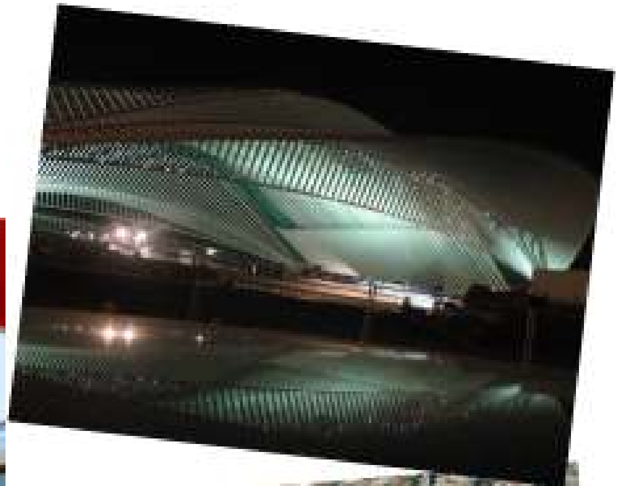

Important centre for Transport & Logistics:

- **2nd river port in Europe**
- **8th freight airport in Europe**

Université de Liège

LGC CHEMICAL ENGINEERING

A collaborative work at LGC (*)

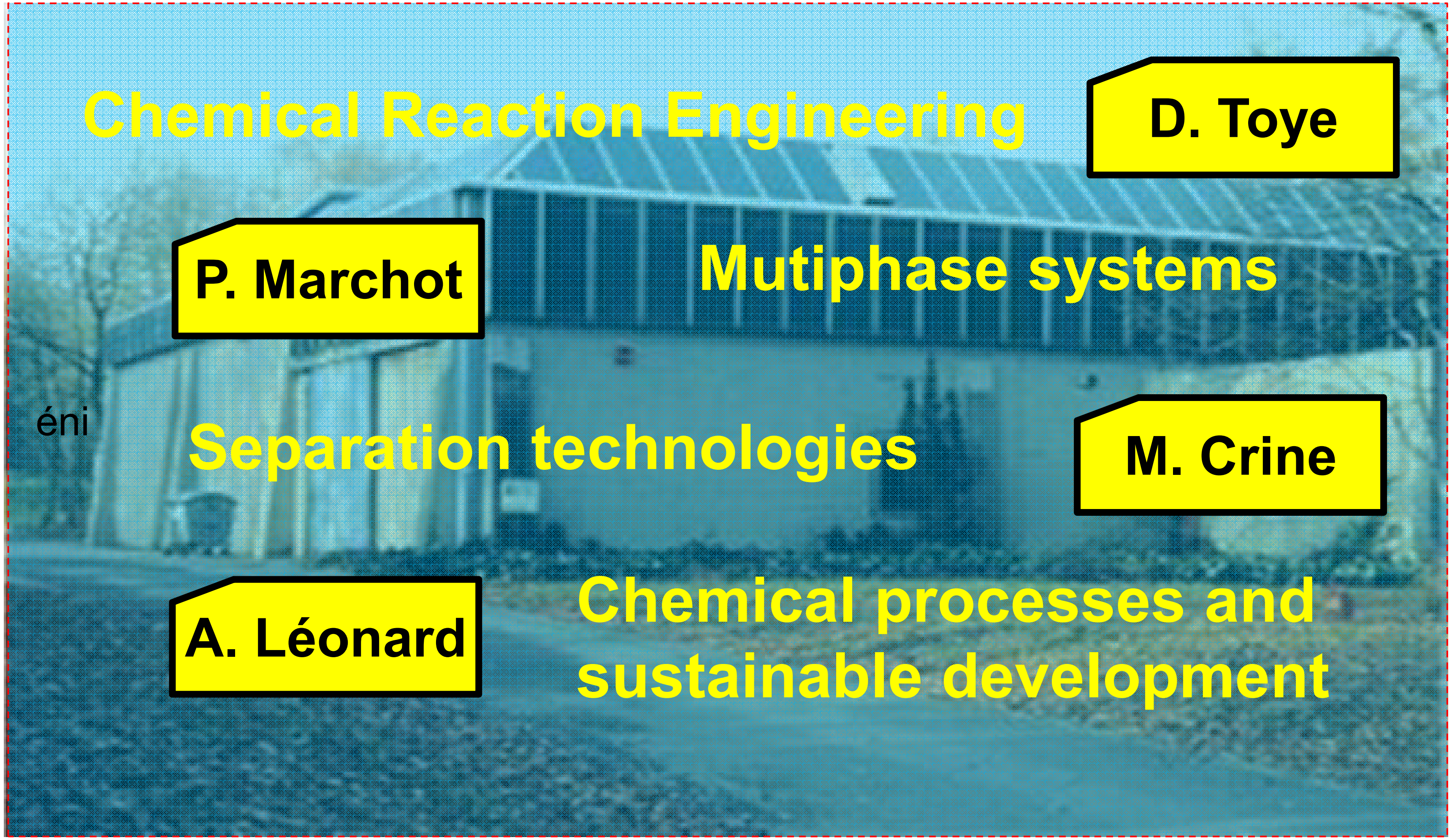

(*) Laboratoire de génie chimique

Flow through porous media

- **A great number of unit operations, e.g.**
  - Fixed bed catalytic reactors
  - Fixed bed adsorbers
  - Fibrous or granular filration systems
  - Packed column absorbers
  - Distillation columns
  - ….

- **Complex (random) porous media whose geometry and texture directly affect fluid flow hydrodynamics.**

- **How to deal with this complexity ?**

Université de Liège

LGC CHEMICAL ENGINEERING

Two objectives:

1. **To get a detailled description of porous media geometry**

   ↳ X-ray (micro)tomographic imaging

2. **To develop a flow simulation model able to deal with the complex geometry of porous media, in terms of boundary conditions**

   ↳ Lattice Boltzmann Methods

X-ray tomography principles

- **Objective**
  - Irradiating an object with X-ray under numerous angles, using a fan beam or a cone beam configuration, to get 2D or 3D images of phase saturation distribution

Fan beam

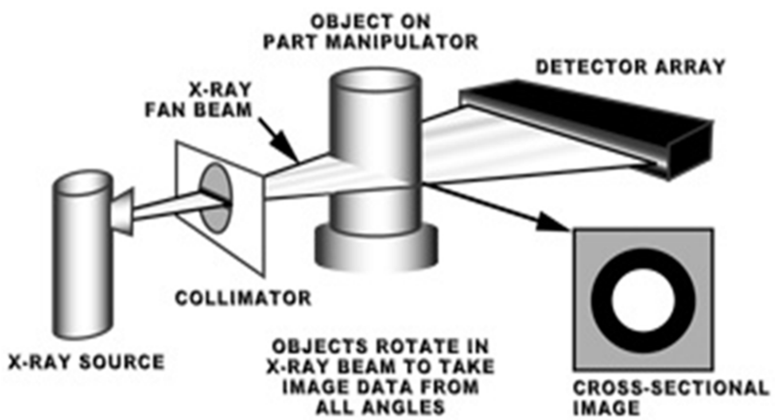

Cone beam

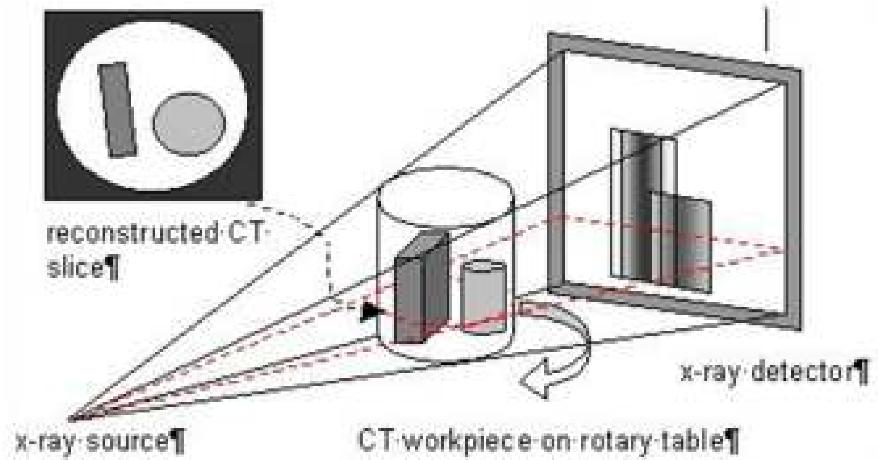

X-ray tomography principles

- **Theory**
  - Visualization technique based on X-ray transmission:

    Beer-Lambert law : $$\frac{dI}{I} = -\mu\, de$$

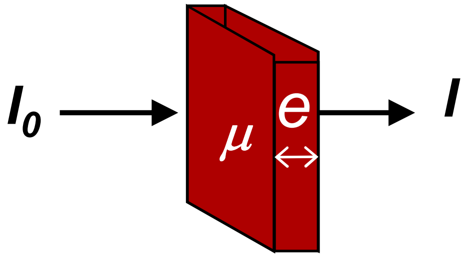

  - μ : attenuation coefficient
    - μ = const.: homogeneous material
    - μ = fct.(e): heterogeneous material

$$\frac{I}{I_0} = \exp(-\mu\, e)$$

$$\frac{I}{I_0} = \exp\left(-\int_e \mu(e)\, de\right)$$

↳ X-ray intensity attenuation along one line depends on local attenuation coefficients values encountered along that line

X-ray tomography principles

- **Values of the attenuation coefficient *μ* depends on:**
  - Material properties
    - the density ρ
    - the atomic number ***Z***
    - the atomic mass ***A***
  - *X-ray* energy ***E***

$$\mu(E) = a\,\rho\,\frac{1}{E^n}\,\frac{Z^m}{A}$$

n and ***m*** depends on X-ray energy range

- At "low" energies: ***m*** = 3.8 ; ***n*** = 3.2
- At high energies ***m*** = 1 ; ***n*** = 1

- ***The most important factors are:***
  - The **density** (gas-solid ; gas-liquid): ρ^{1}
  - The **atomic number** ~ Z^{2} (at low energies, *Z/A ~ Const.)*

X-ray tomography applications

- **X-ray tomography allows differentiating elements with strong differences in density, e.g.:**

Gas and solid in porous material (deer antlers)

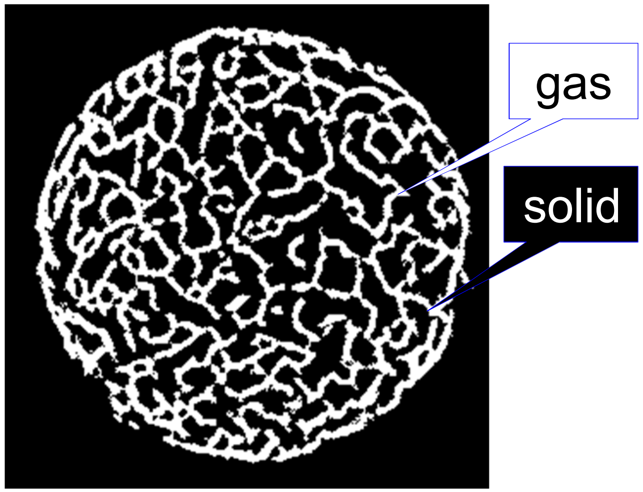

Léonard et al.(2007).
Journal of Microscopy-Oxford 225(Pt 3), 258-263

Gas and liquid in gas-liquid contactors

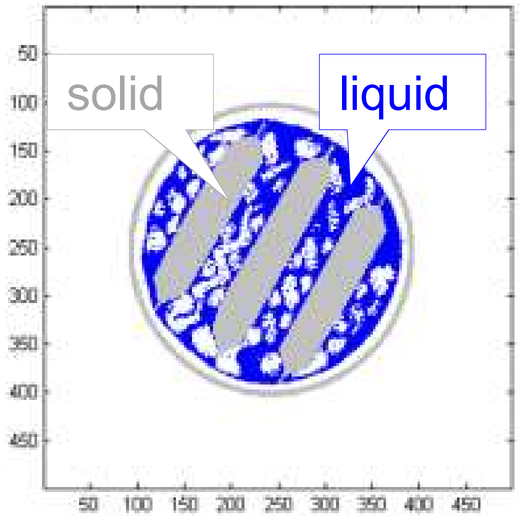

Aferka et al.(2010).
Canadian Journal of Chemical Engineering *88*(4), 611-617

X-ray tomography applications

- **X-ray tomography also allows differentiating elements according their atomic numbers *Z*, e.g.:**
  - Adsorption of methyliodide (CH_3I ; Z_I = **53**) on activated carbon (Z_C = **6**) in a gas mask filter (coll. Royal Military Academy)

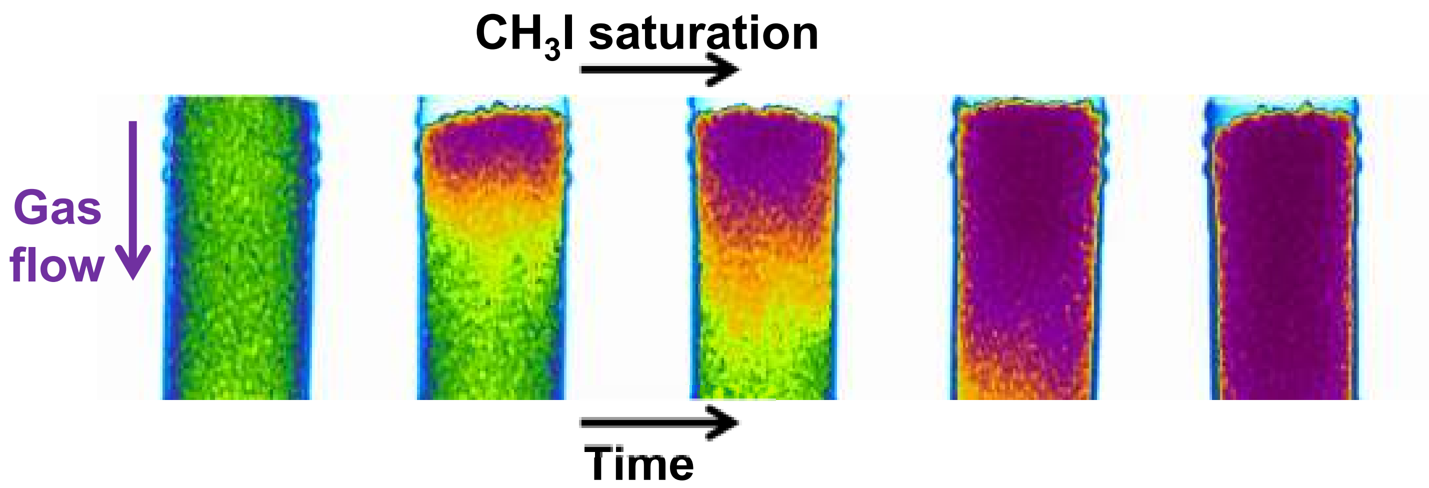

Verdin, et al. (2010). 7th European Congress of Chemical Engineering (ECCE7), Prague

Tomographic image reconstruction

- **Back projection algorithm**

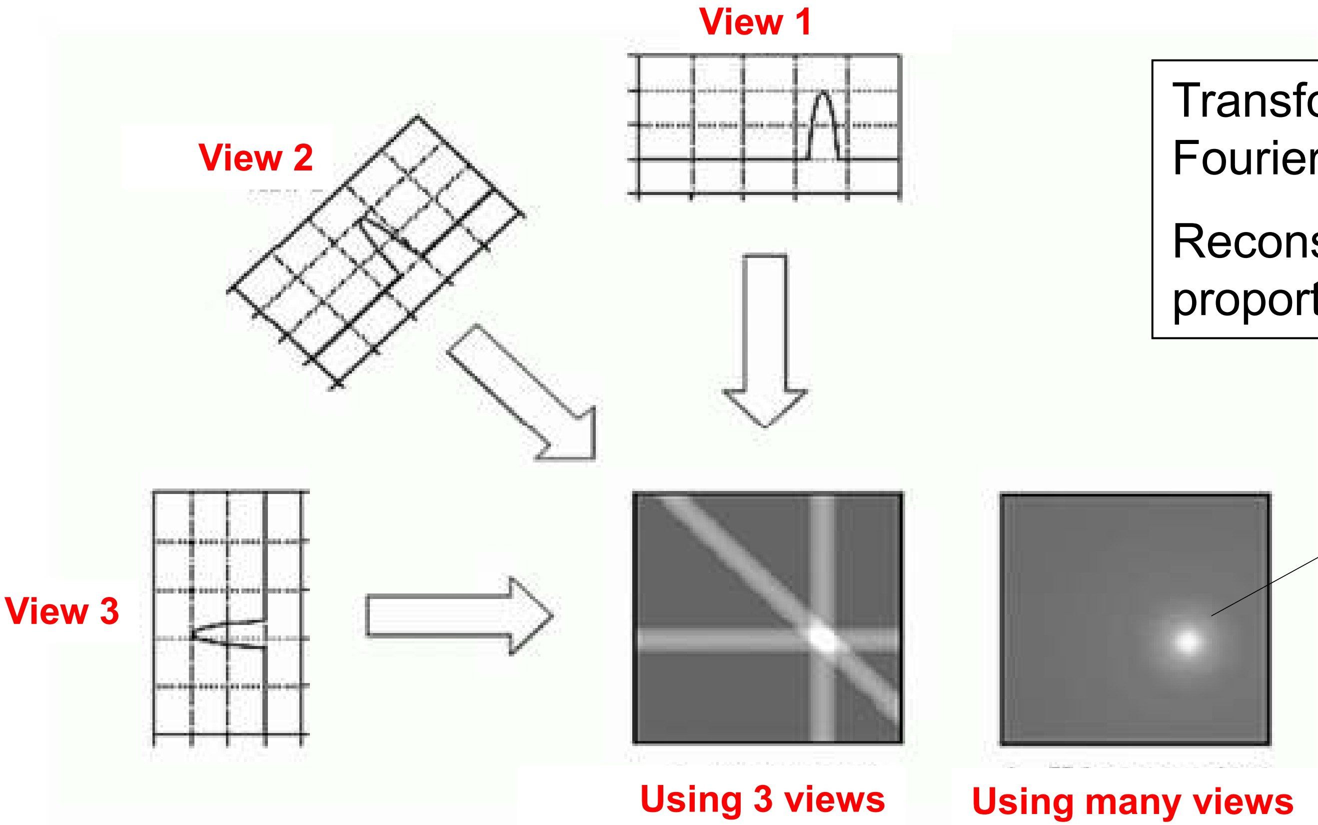

Transformation in the Fourier domain

Reconstruction time proportional to N^3

Blurred image

Tomographic image reconstruction

- **Filtered back projection algorithm**

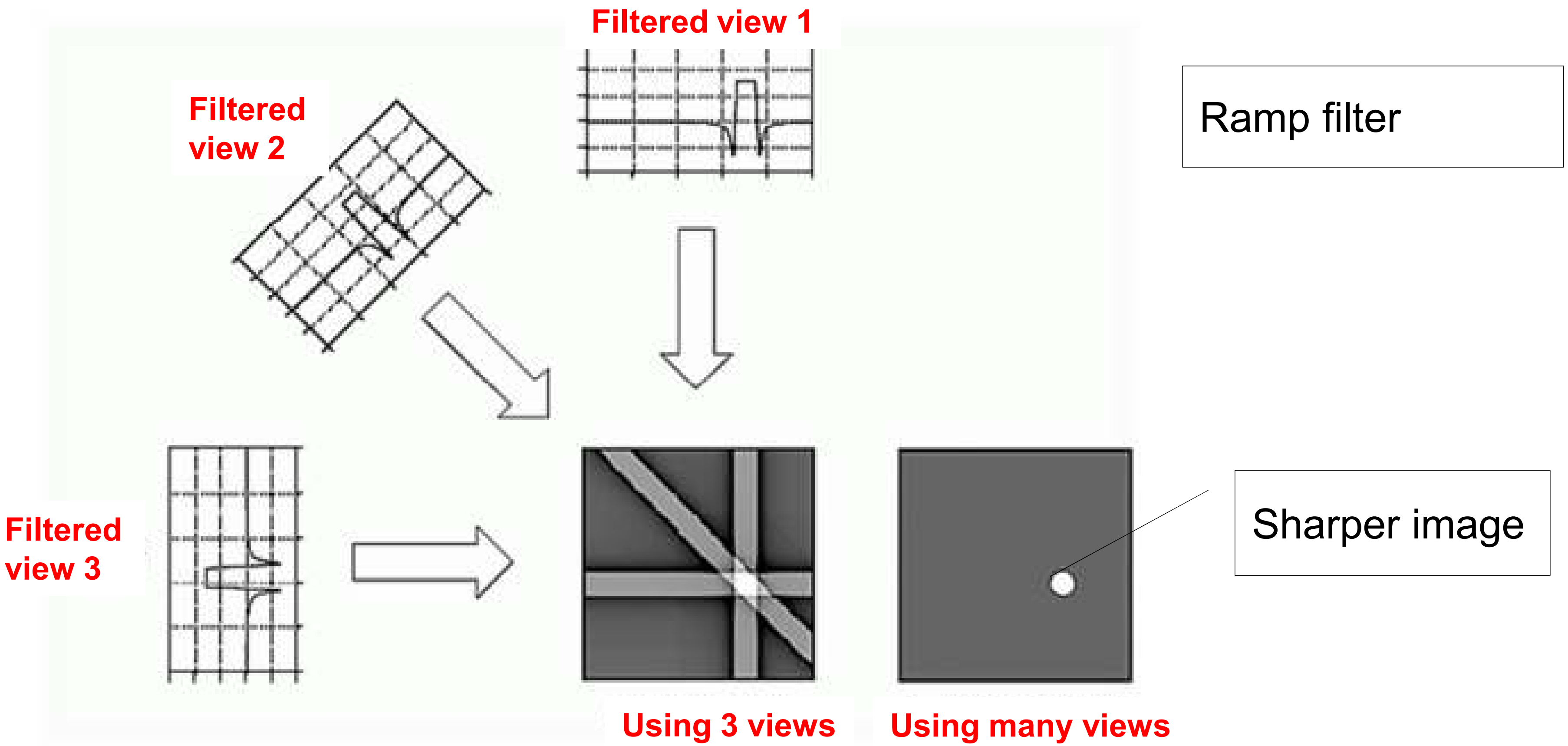

Microtomographic equipments

- **High resolution (a few microns) visualization of small size (a few centimeters) objects**
- **Several commercial microtomographs, e.g. :**
  - High resolution tomograph Skyscan 1172 (Skyscan, BE)
    - **<u>X-ray ray source</u>**

      Microfocus
      Voltage : 20-100 kV
      Curent : 0-250 mA
      Cone beam geometry

    - **<u>Detector</u>**

      High resolution CCD camera (10 Mpixels)
      Pixel size: from 2 to 35 µm

Université de Liège

LGC CHEMICAL ENGINEERING

Microtomographic equipments

- **A wide range of spatial resolutions and X-ray energies**

Microtomograph	2 – 40 µm	30 – 200 keV
Synchrotron microtomograph	≅ 0.3 µm	6 – 150 keV
Nanotomograph	≅ 100 nm	20-80 keV

- **A lot of applications**
  - Material sciences
  - Electronics
  - Biomedical
  - Agrofood
  - Geology
  - ….

Skyscan, Kontich, BE
http://www.skyscan.be

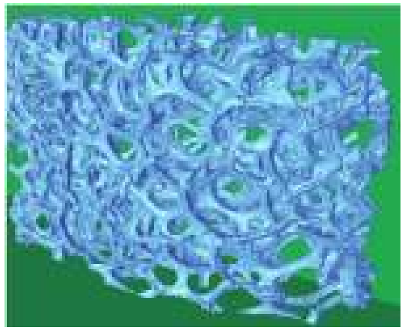

Nickel foam

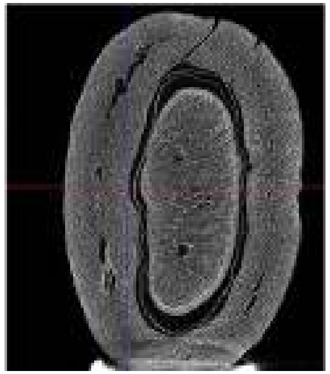

Coffee bean

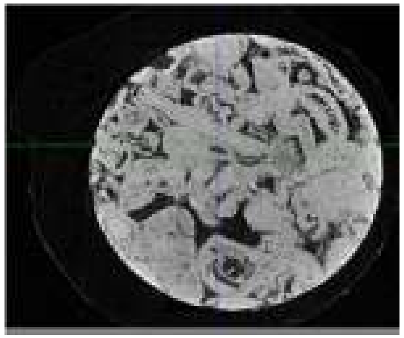

Rock

Université de Liège

LGC CHEMICAL ENGINEERING

Macrotomographic equipments

- **Macrotomography or 'industrial' tomography aims at visualizing much larger objects, e.g. unit operations.**

- **No commercial standard equipment**
  - An example : the high energy tomographic facility available at the LGC
  - Main applications : visualizing hydrodynamics in distillation and gas-liquid absorption columns

e.g. ; Aferka, et al. (2010) *Chemical Engineering Science*, *65*(1), 511-516.

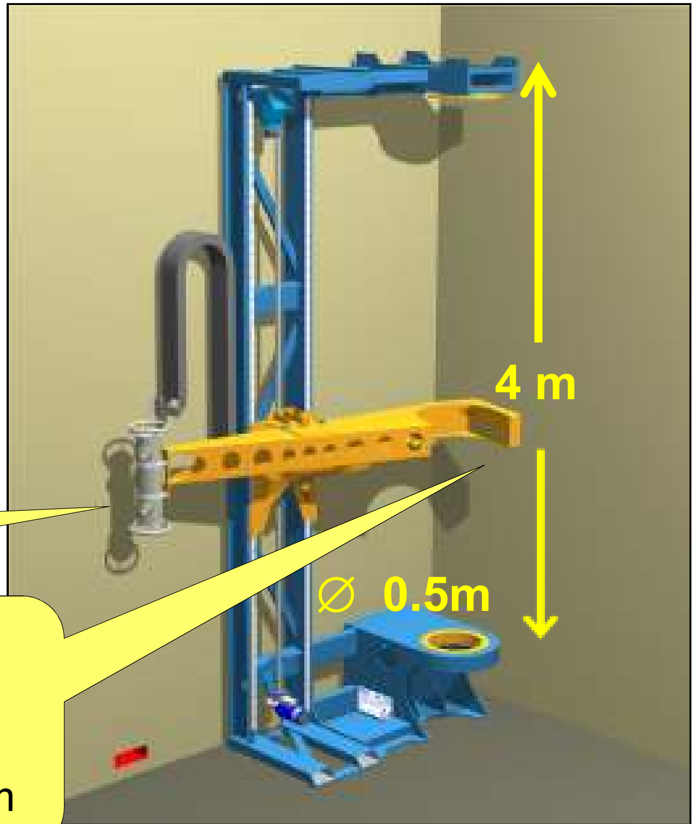

X-ray ray source

Focal spot : 0.8 mm

Voltage : 30-420 kV

Curent : 2-8 mA

Fan beam geometry (40°)

Linear detector

1280 photodiodes

Pixel size: ~ 0.3 mm

A few macrotomographic images

- Gas-liquid distribution in a catalytic distillation Packing (Katapak™ SP12, Sulzer Chemtech, CH)

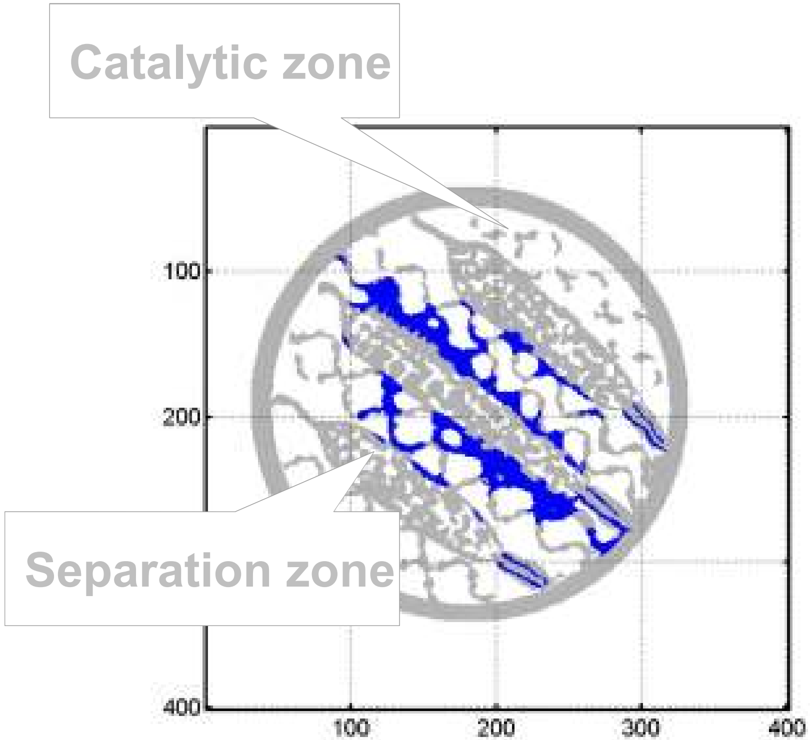

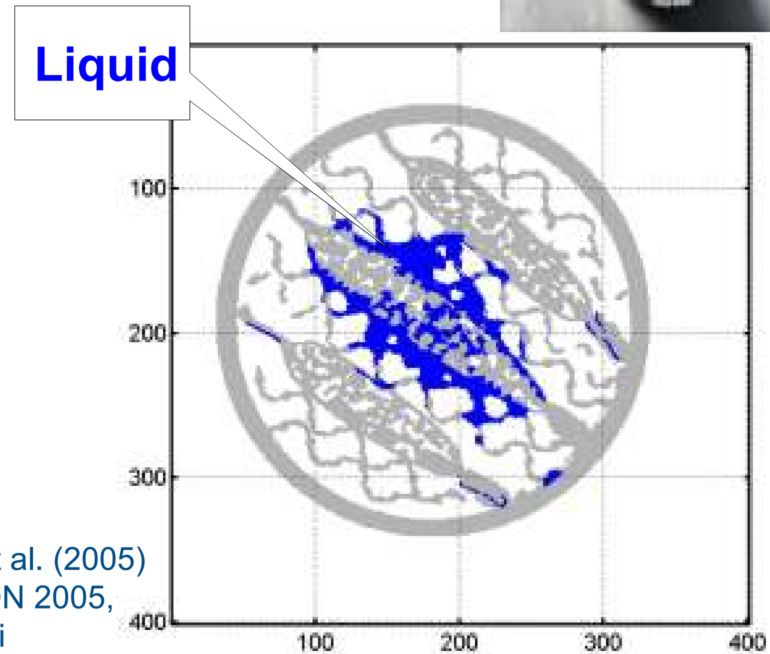

Aferka, et al. (2005)
CHEMCON 2005,
New Delhi

A few macrotomographic images

- Gas-liquid distribution in a structured packing
  (Mellapak Plus™ 752Y , Sulzer Chemtech, CH)

Liquid

Corrugated sheet

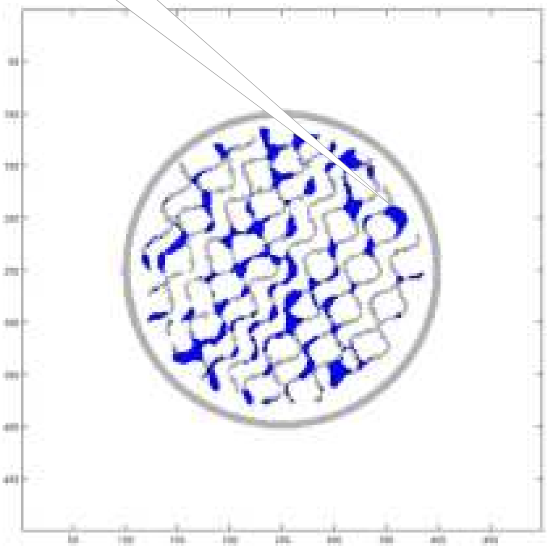

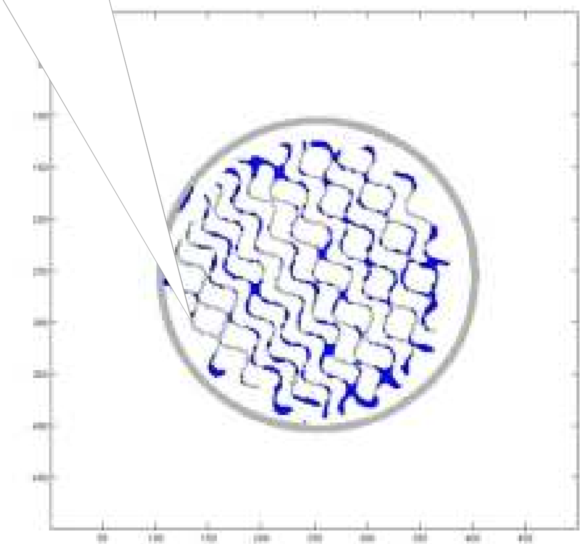

(Macro)tomographic applications

- Large scale high energies tomographic facilities available, a.o., at:
  - *Helmholtz-Zentrum Dresden-Rossendorf (DE)* (X-ray)
  - *University of Texas at Austin (USA)* (X-ray)
  - *IIT Delhi (IN)* (gamma-ray)
  - *IFP-EN (FR)* (gamma-ray)
  - *Missouri University of Science and Technology* (gamma ray)
  - *University of Washington St Louis (USA)* (gamma ray)

Image analysis: a first example

- **Structure visualization of a open cell metallic foam**

  (RCM-NCX-1116 of RECEMAT® International, NL)

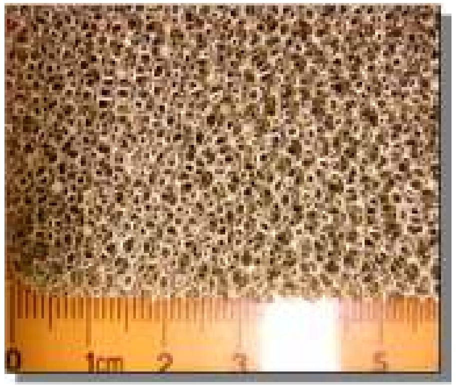

  - Material: Nickel – Chromium deposited onto open-cell polyurethane foam
  - Mean pore diameter: 1.4 mm
  - Grade number: 11 – 16 ppi
  - Specific area: 1000 m^2/m^2
  - Porosity: ~ 95 %
  - Density: ~ 0.6 g/cm^3

2D images processing

Hollow strut

« Filled » strut

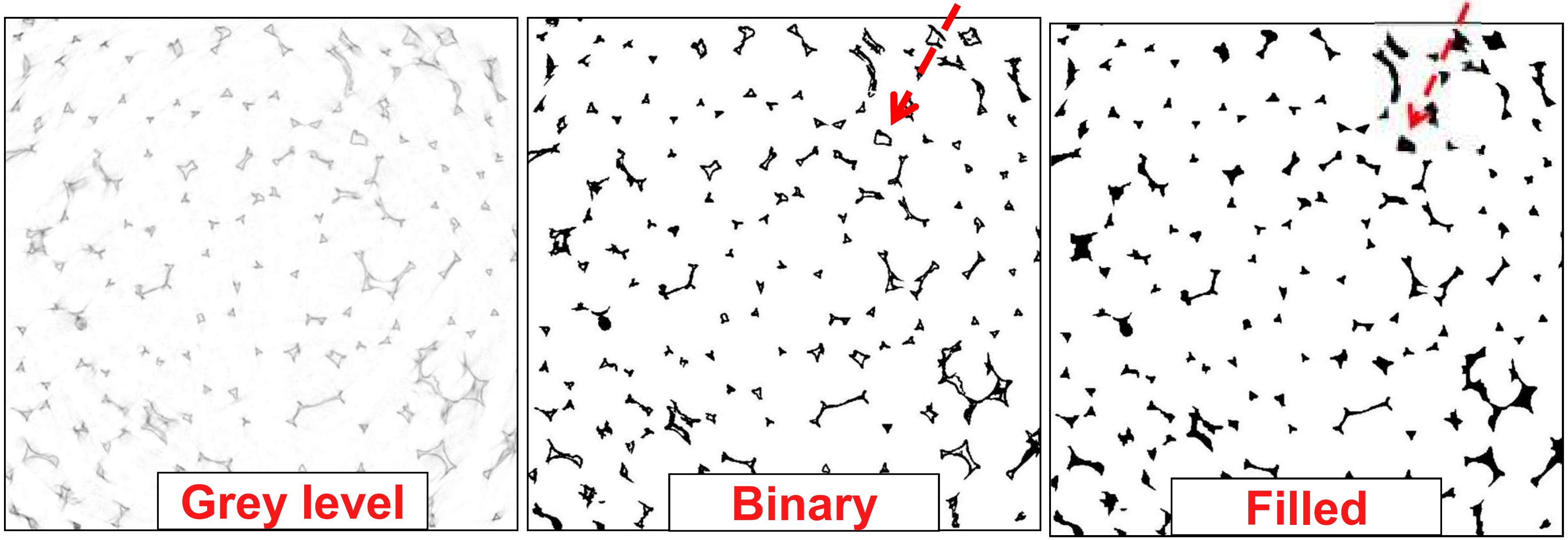

Thresholding + Binarization + Erosion → **Internal « porosity » filling** →

3D images processing

- **<u>3D imaging</u>**
  - 3D images are obtained by stacking a series of 2D cross sections
  - The grey level image is obtained by adding shadow effects on the binary image

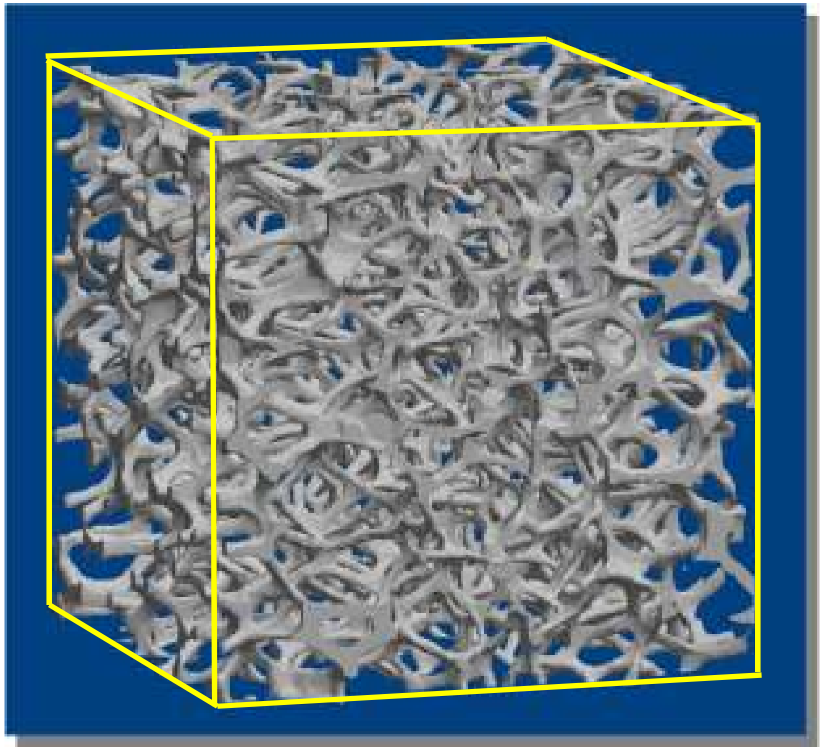

Image analysis: a second example

- **Visualization of a structured packing used in absorption columns**

  (Mellapak Plus™ 752Y of Sulzer Chemtech, CH)

  - ◻ Material: Embossed, perforated corrugated sheets of stainless steel
  - ◻ Element height : 0.2 m
  - ◻ Element diam. : 0.09 m
  - ◻ Specific surface area : 510 m^{-1}
  - ◻ Void fraction : 97.5 %

2D images processing

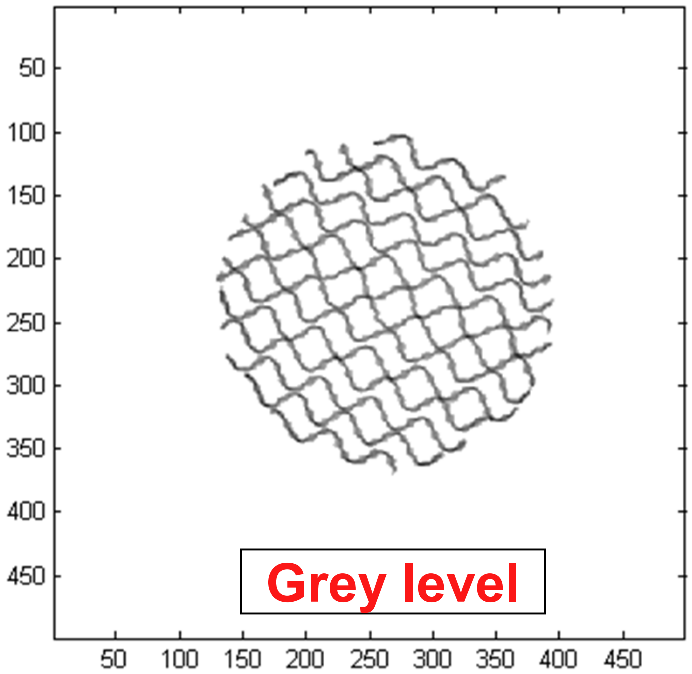

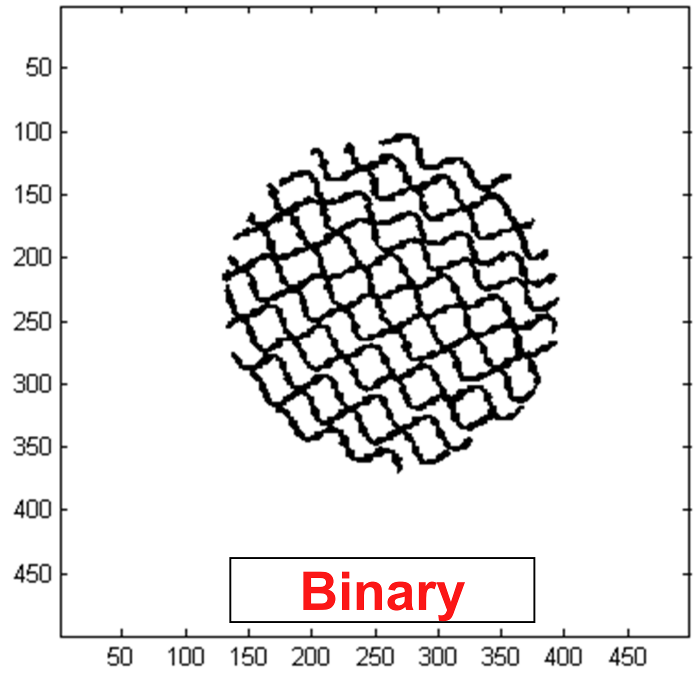

Thresholding
+
Binarization

Two objectives

1. To get a detailled description of porous media geometry

A 3D binary (gas-solid) matrix

↳ X-ray (micro)tomographic imaging

2. **To develop a flow simulation model able to deal with the complex geometry of porous media, in terms of boundary conditions**

↳ Lattice Boltzmann Methods

Lattice Boltzmann Models

- Fluid flow is represented by the movement of fictitious particles allowed to **move** and **collide** on a lattice.

.

- A triple discretization
  - Space → Lattice
  - Velocity or momentum
  - Time

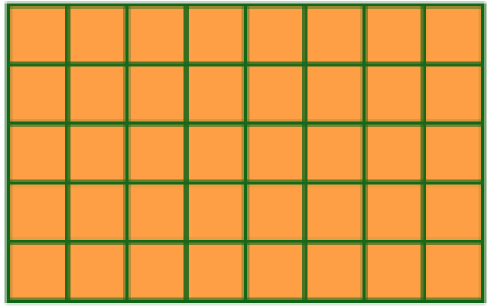

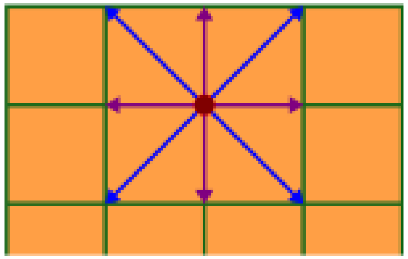

Lattice Boltzmann Models

- The particles jump from one lattice node to the next, according to their (discrete) velocity.
  - *This is the **propagation phase**.*
- Then, the particles collide and get a new velocity.
  - *This is the **collision phase**.*
- Rules governing the collisions are designed such that the time-average motion satisfies mass and momentum conservation

Adequate lattices

- A limited number of lattices are able to cope with this constraint, e.g. :

2D : D2Q9
2 dimensions, 9 velocities

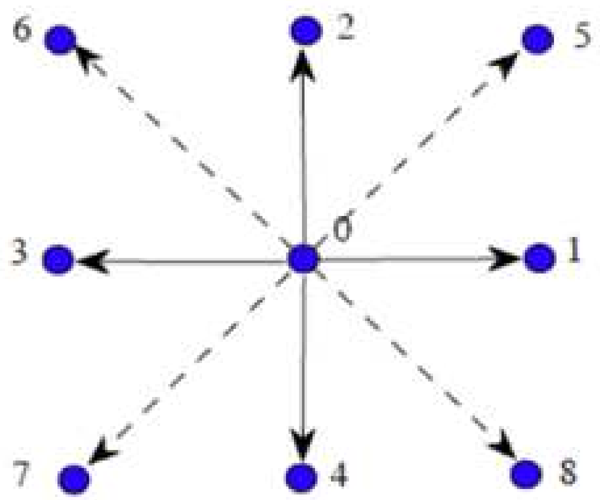

3D : D3Q19
3 dimensions, 19 velocities

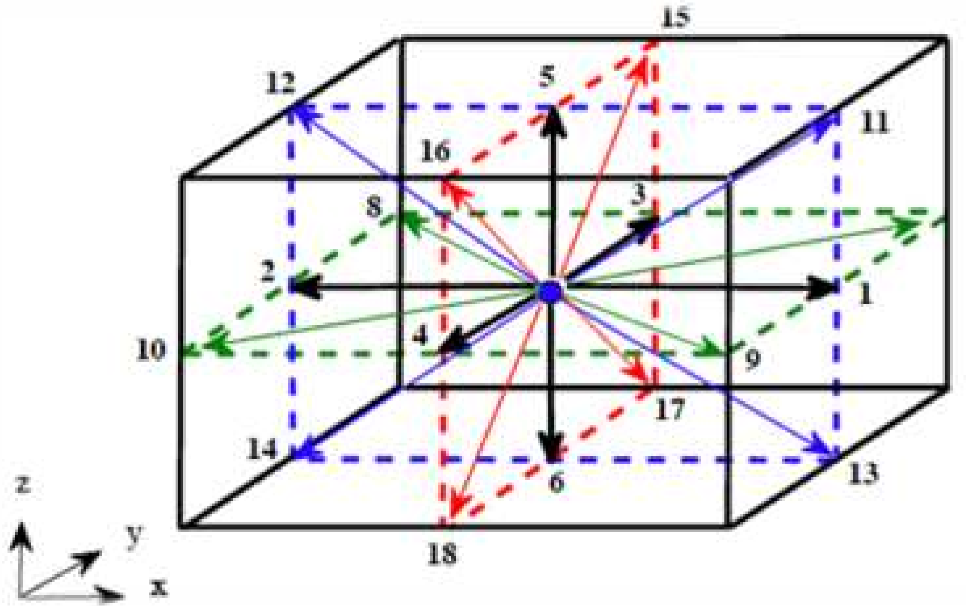

Kinetic equation of evolution

- Particle occupation within the lattice is described by a series of particle density distribution functions f_k
- The evolution of these functions is described by a discrete form of the Boltzmann equation

$$\boxed{\tilde{f}_k(x,t) = f_k(x,t) + \Omega_k(x,t), \quad k = 0,\ldots,q-1}$$

q : number of directions

- Ω_k is the collision operator : it determines the way velocities are modified after each collision

Collision operator

- Different ways to determine the collision operator.
- They all describe a relaxation process towards equiibrium
  - **SRT:** single relaxation time approximation

    Bhatnagher-Gross-Kook (BGK) collision model

$$\Omega_k^{BGK}(f) = -\frac{1}{\tau}(f_k - f_k^{(eq)}).$$

  - **MRT:** multiple relaxation times approximation

$$\Omega_k^{MRT}(x,t) = -\mathbf{M}^{-1}\widehat{\mathbf{R}}\left[\mathbf{m}(x,t) - \mathbf{m}^{(eq)}(x,t)\right].$$

Université de Liège

LGC CHEMICAL ENGINEERING

Simulation algorithm

- 3D tomographic binary image (matrix)

- $f_k(x + e_k\delta_t,\ t + \delta_t) = \tilde{f}_k(x, t), \quad k = 0, \ldots, q-1$

- $\tilde{f}_k(x, t) = f_k(x, t) + \Omega_k(x, t), \quad k = 0, \ldots, q-1.$

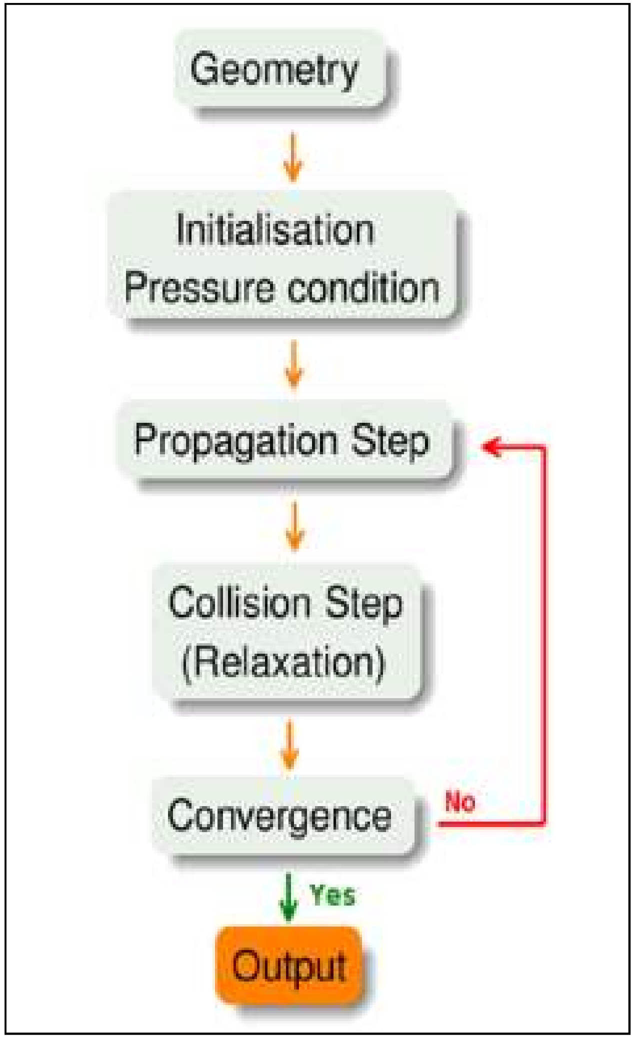

Boundary conditions

- Pressure gradient between the entrance and exit faces

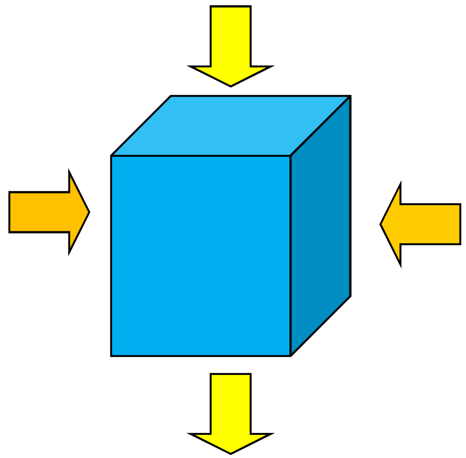

- Periodic boundary conditions on faces parallel to the flow direction

- Bounce back conditions (no slip) at the fluid-solid interface

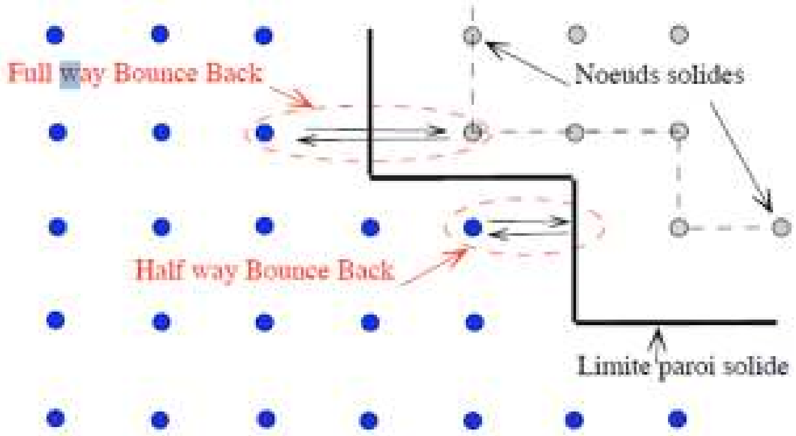

Lattice units conversion

- LB simulations are expressed in lattice units
- The comparison with real systems implies to convert LB units into real (physical) units.
- The conversion is rather tricky and different ways have been proposed.
- A guideline : dimensionless variables, e.g., Reynolds number are conserved.

$$\underbrace{Re_{Phys.} = \frac{u_{phys}\, d}{\nu_{phys}}}_{\text{«Physical» world}} = \underbrace{Re_{LB} = \frac{u_{LB}\, d_{LB}}{\nu_{LB}}}_{\text{«LB» world}}$$

ν_{LB} represents the kinematic viscosity in the LB domain.

It is fixed according to the value of the relaxation parameter τ

A few examples of flow simulation

- Through a metallic foam
- Through an activated carbon fixed bed
- Through a fiber filter
- Through a structured packing

Flow through a metallic foam

- **Open cell metallic foam**
  (RCM-NCX-1116 of RECEMAT® International, NL)

  - Material: Nickel – Chromium
  - Mean pore diameter: 1.4 mm
  - Grade number: 11 – 16 ppi → Pore aperture ~ 1.6 – 2.3 mm
  - Specific area: 1000 m^2/m^2
  - Porosity: ~ 95 %
  - Density: ~ 0.6 g/cm^3

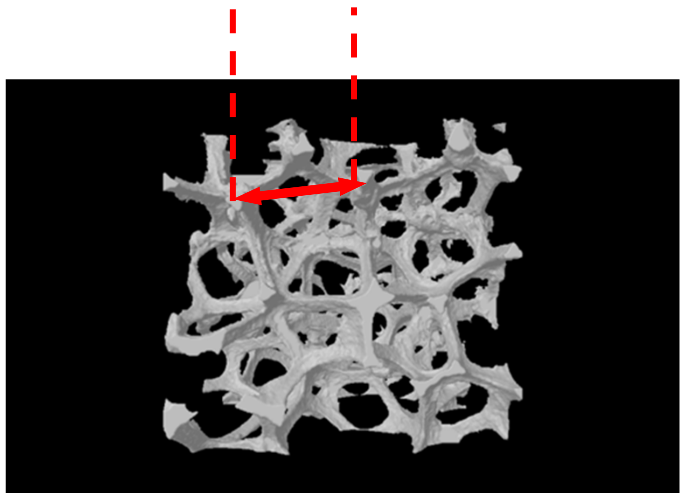

Beugre et al, 2009,
Journal of Computational & Aoolied Mechanics
.

3D imaging of the porous texture

- Sample size
  - 176 × 176 × 352 voxels ~ 11 × 11 × 22 mm
  - 1 voxel ~ 64 × 64 × 64 μm^3
  - Porosity: ~ 95 %

2D image

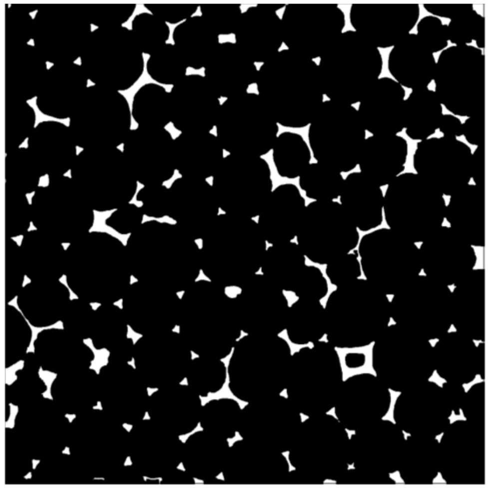

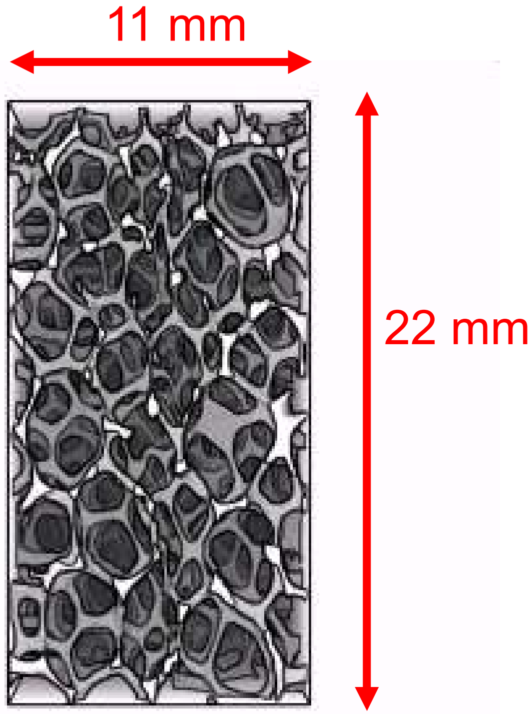

By stacking a series of 2D images

2D Flow visualization

- Velocity distribution in a plane perpendicular to the flow direction.

Moving along the flow direction : 54 images

Preferential flow paths

« Strut »

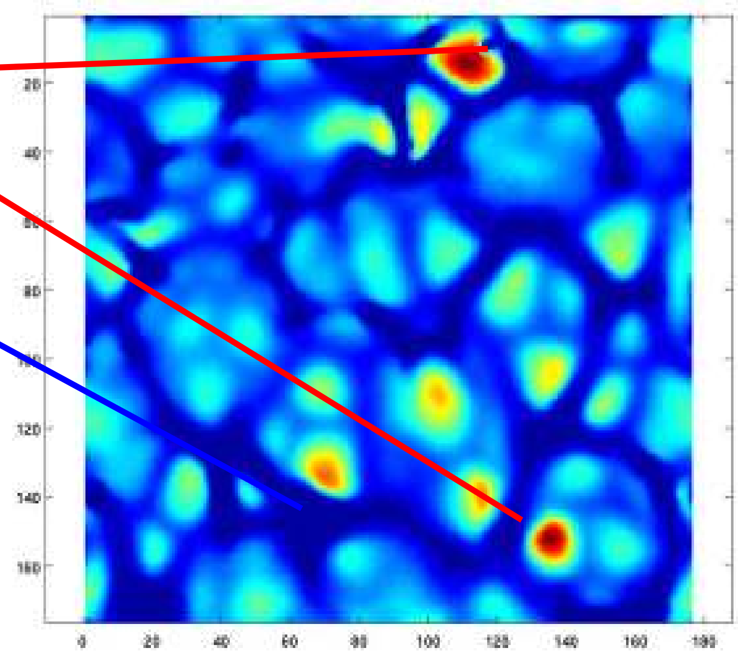

- Simulation conditions
  - **D3Q19**
  - **SRT** (BGK) collision mode
  - **B.C.** : - Pressure gradient

    - Periodic boundary cond.

    - Full bounce back (no slip)

Université de Liège

LGC CHEMICAL ENGINEERING

3D Flow visualization

- Simulation conditions
  - **D3Q19**
  - **SRT** (BGK) collision mode
  - **B.C.** : - Pressure gradient

    - Periodic boundary cond.

    - Full bounce back (no slip)

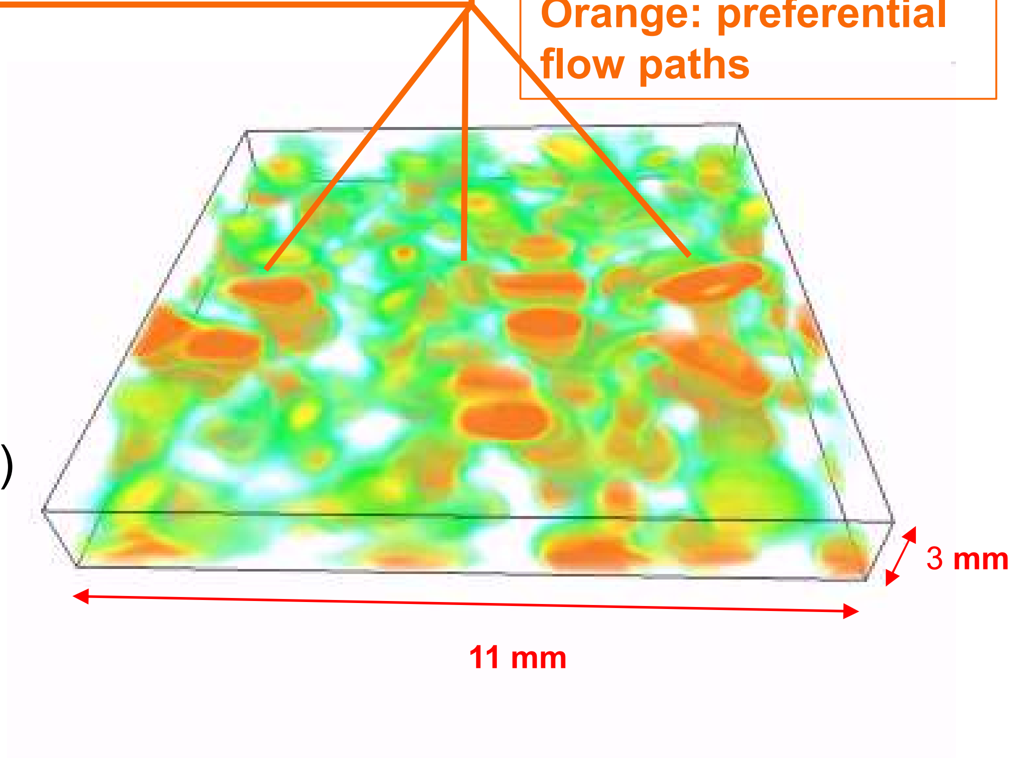

Pressure drop

$$\frac{\Delta P}{L} = \frac{\rho}{d_P} \frac{(1-\varepsilon)}{\varepsilon^3} \left[A \frac{(1-\varepsilon)}{Re} + B \right] \cdot u_{\mathrm{sup}}^2$$

Ergun equation fitted on LB numerical simulations

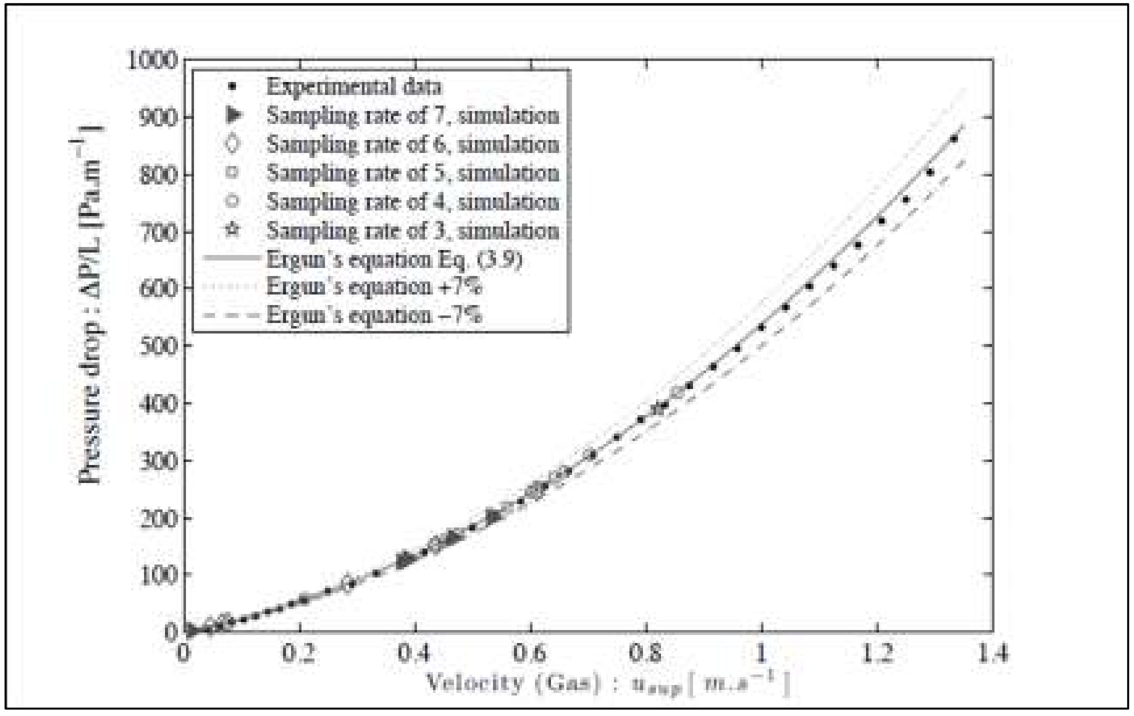

A = 77.9
B = 0.77

A few examples of flow simulation

- Through a metallic foam
- Through an activated carbon fixed bed
- Through a fiber filter
- Through a structured packing

Flow through activated carbon

- Activated carbon granules synthetised from recycled PET bottles

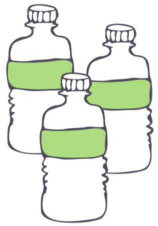

PET
bottles

Pyrolysis

700 ºC, N_2+ 925 ºC, N_2, 1 h

Carbon particles

Crushing

Sieving

Granulometry between
1 and 1.5 mm

Activation

925 ºC, CO_2

Irregularly shaped particles

2D imaging of the porous texture

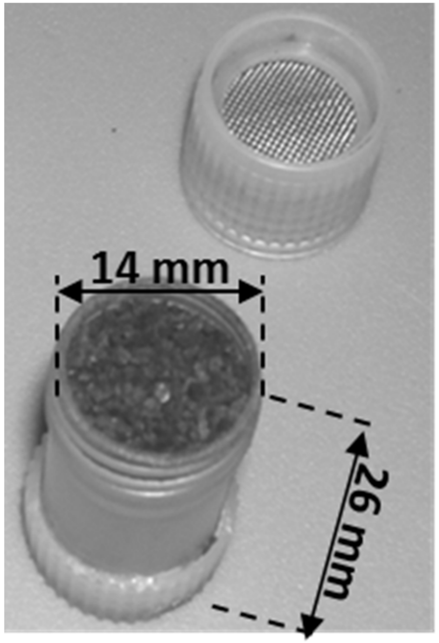

Images of cross-sections at three different depths separated by 2 mm

Solid : white zones

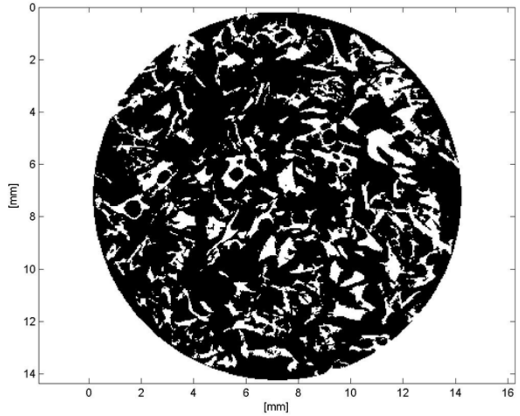

Bed porosity : ~ 78 %

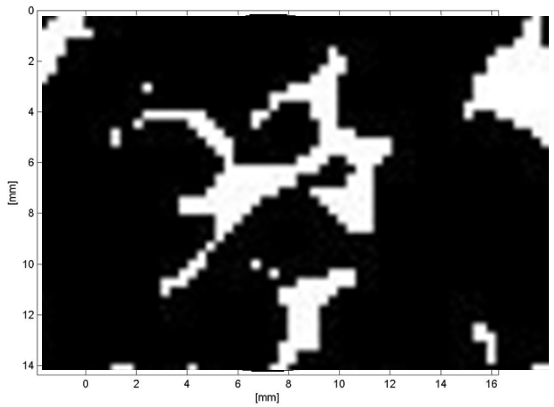

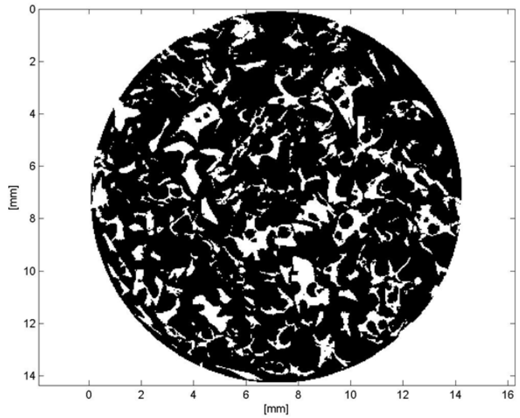

- Sample size
  - Diam. : 14 mm
  - 1 pixel ~ 40 × 40 μm^2

Verdin et al, 2010
FOA10, 10th Internationnal Conference on Fundamentals of adsorption

3D imaging of the porous texture

1 voxel ~ $10 \times 10 \times 10\ \mu m^3$

CA: Brown zone

2D Image

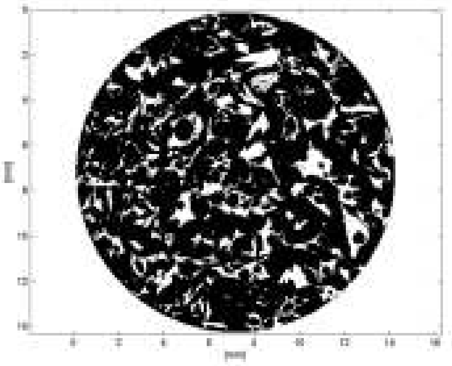

By stacking a series of 2D images

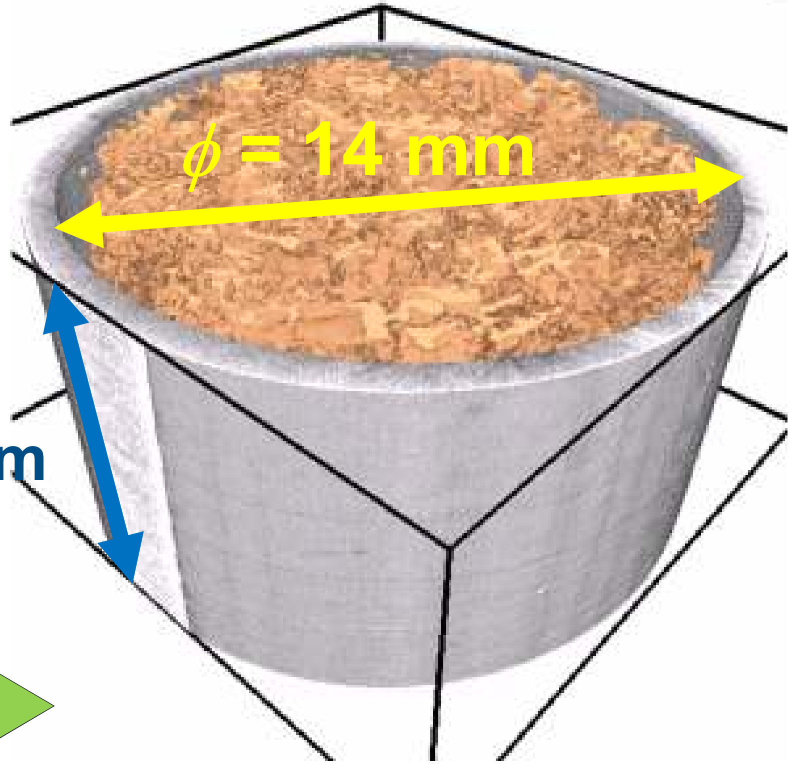

Flow visualization

Solid : white zones

- Simulation conditions
  - **B.C. :** - Pressure gradient

    - Periodic boundary conditions

    - Full bounce back (no slip)
  - **D3Q19**
  - **SRT** (BGK) collision mode

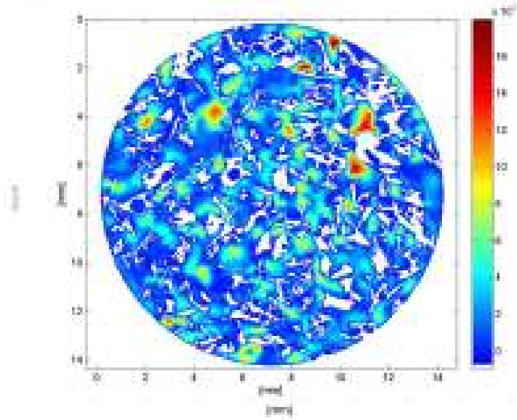

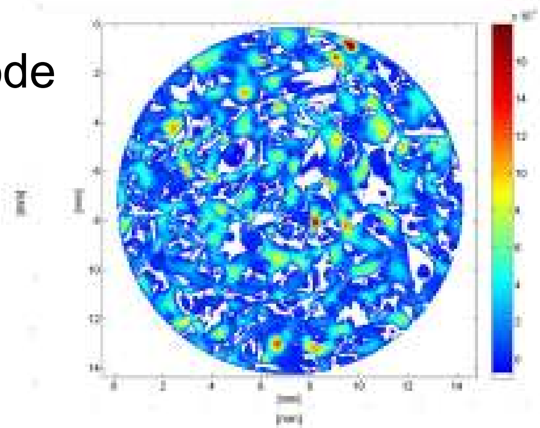

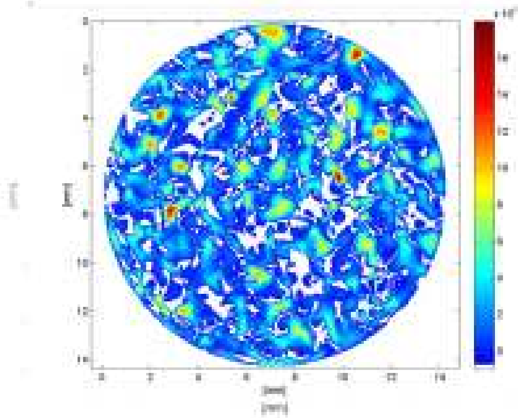

- Sample size
  - Diam. : 14 mm
  - 1 pixel ~ 40×40 µm^2

Pressure drop

$$\frac{\Delta P}{L} = \frac{\rho}{d_P}\frac{(1-\varepsilon)}{\varepsilon^3}\left[A\frac{(1-\varepsilon)}{Re} + B\right]\cdot u_{\text{sup}}^2$$

Ergun equation fitted on LB numerical simulations

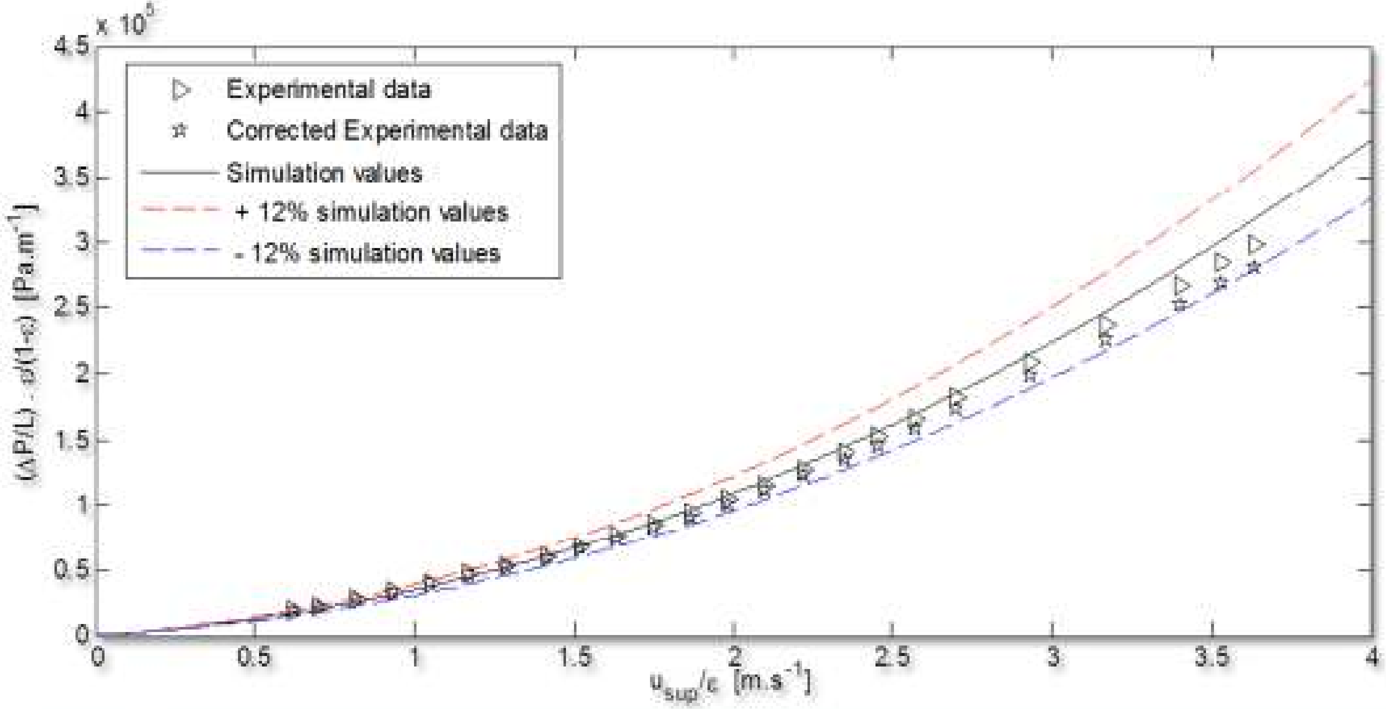

A = 4887
B = 25

Université de Liège

A few examples of flow simulation

- Through a metallic foam
- Through an activated carbon fixed bed
- Through a fiber filter
- Through a structured packing

Flow through a fibre filter

- High permeability fibre filtration media
  (PST 290 of ACS Filter Mechelen, BE).

  - Material: Polyester
  - Grade number: G3 (EN 779)
  - Fiber diameter: ~ 20 µm
  - Porosity: ~ 98 %

3D tomographic view

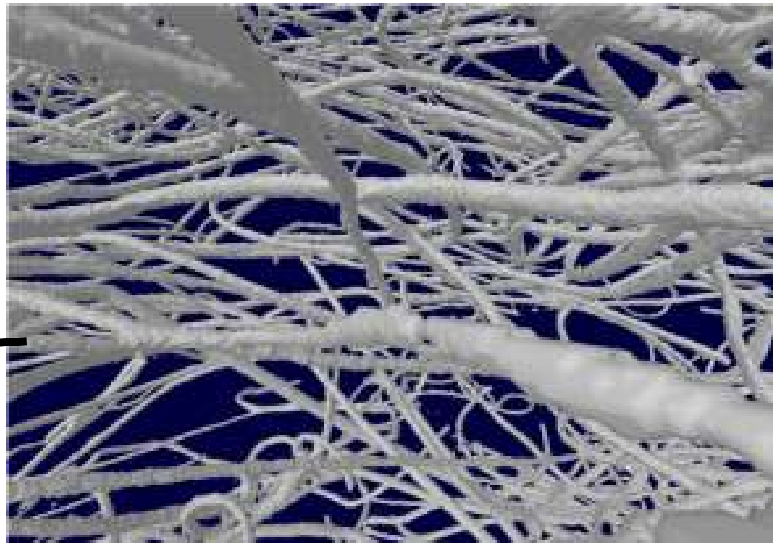

2D imaging of the porous texture

- Sample size
  - 358 x 358 x 200 voxels
  - 1 voxel ~ 20 × 20 × 20 µm^3

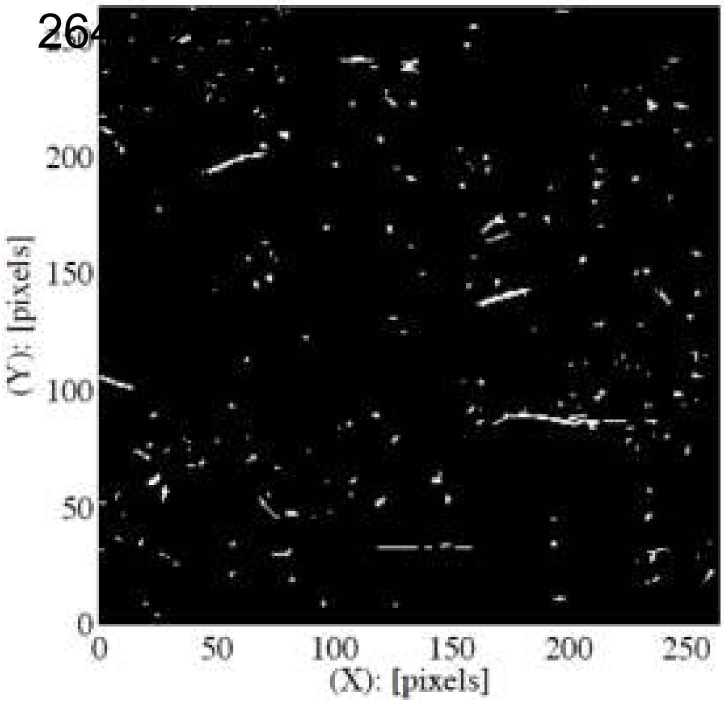

Z = 20 µm

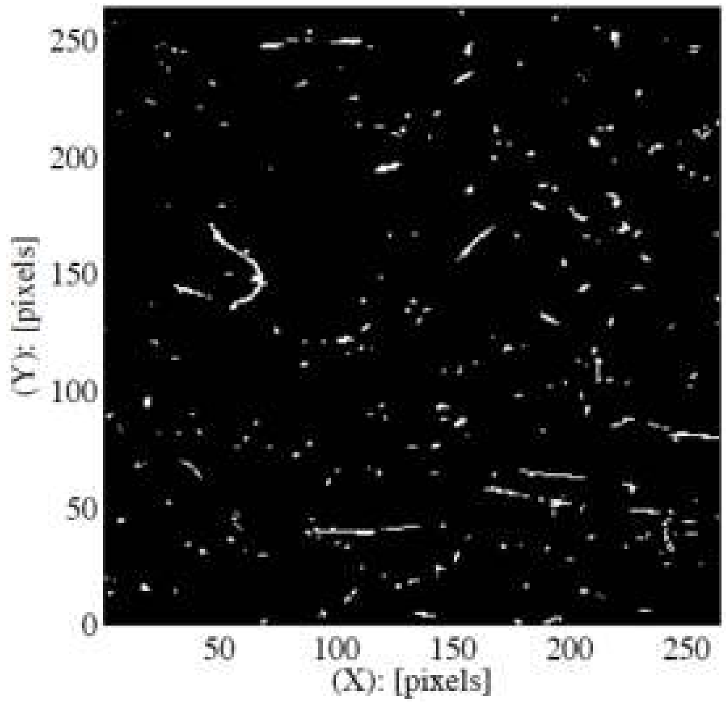

Z= 1 mm.

Flow visualization

- Flow distribution within a series of cross-sections **Re ~ 1**
  - *From the inlet of the gas flow (Z= 20 µm) towards the outlet (→ Z = 3 mm) of the filter*

Max. velocity

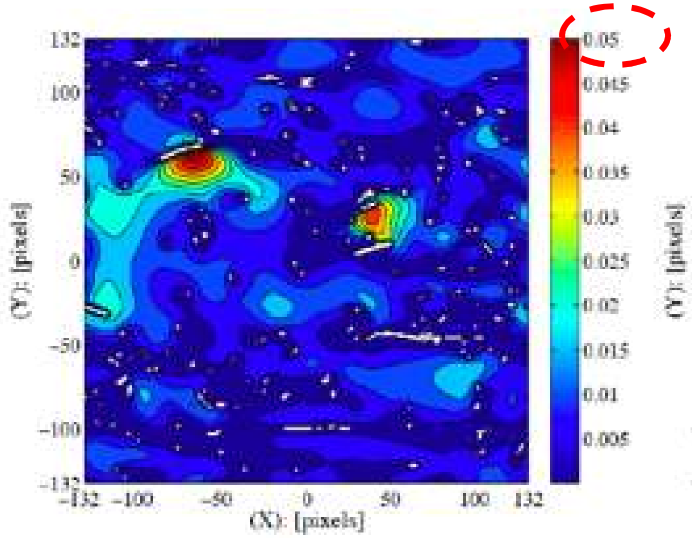

Z = 20 µm

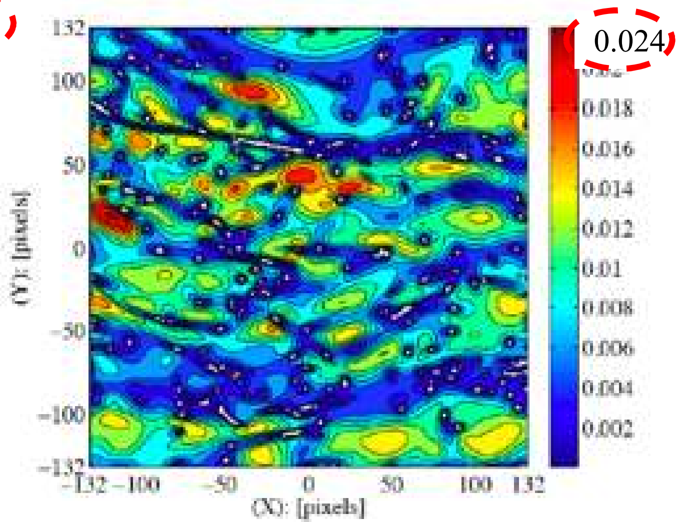

Z = 3 mm

- Spreading of the gas flow within the filter cross-section
- Decrease of the maximum velocity

Université de Liège

LGC CHEMICAL ENGINEERING

Pressure drop

$$\frac{\Delta P}{L} = \frac{\rho}{d_P}\frac{(1-\varepsilon)}{\varepsilon^3}\left[A\frac{(1-\varepsilon)}{Re} + B\right]\cdot u_{sup}^2$$

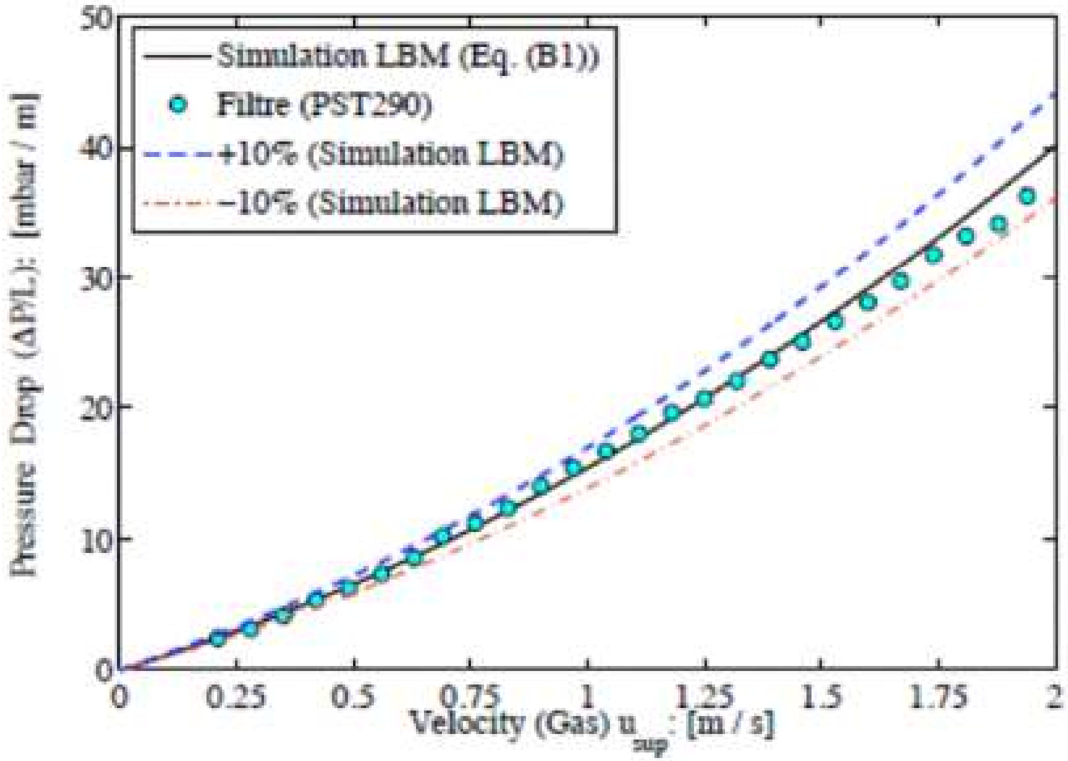

Ergun equation fitted on LB numerical simulations

A = 46.2
B = 0.35

Université de Liège

LGC CHEMICAL ENGINEERING

Permeability of porous media

- Computed permeability

$$K = \frac{\varepsilon^3 \, {d_P}^2}{A\,(1-\varepsilon)^2}$$

	ε (-)	d_P (m)	A (-)	**K (m^2)**	
Metallic foam	0.95	$1.4\ 10^{-3}$	77.9	**$5.38\ 10^{-8}$**	Max. permeanility
Activated carbon	0.78	$1.25\ 10^{-3}$	4887	**$3.07\ 10^{-9}$**	Min. permeability
Fibre filter	0.98	$6.5\ 10^{-4}$	46.2	**$2.02\ 10^{-8}$**	Less permeable than foam

A few examples of flow simulation

- Through a metallic foam
- Through an activated carbon fixed bed
- Through a fiber filter
- Through a structured packing

Flow through a structured packing

- **Flow between two corrugated sheets of a structured packing**
- **Structured packing**

  Sulzer Plastic MellapakTM 250 Y, Sulzer ChemTech, CH

  - Material: Polyethylene
  - Hydraulic diam. : 2 cm
  - Corrugation geometry
    - Triangular channel base : $b_0 = 26mm$
    - Triangular channel height : $h = 13mm$
  - Specific area: 250 m^2/m^2
  - Porosity: ~ 85 %

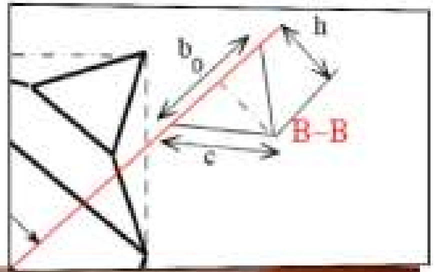

3D geometry modelling

- Two corrugated sheets of Mellapak 250 Y containing four triangular channels each (without perforation)

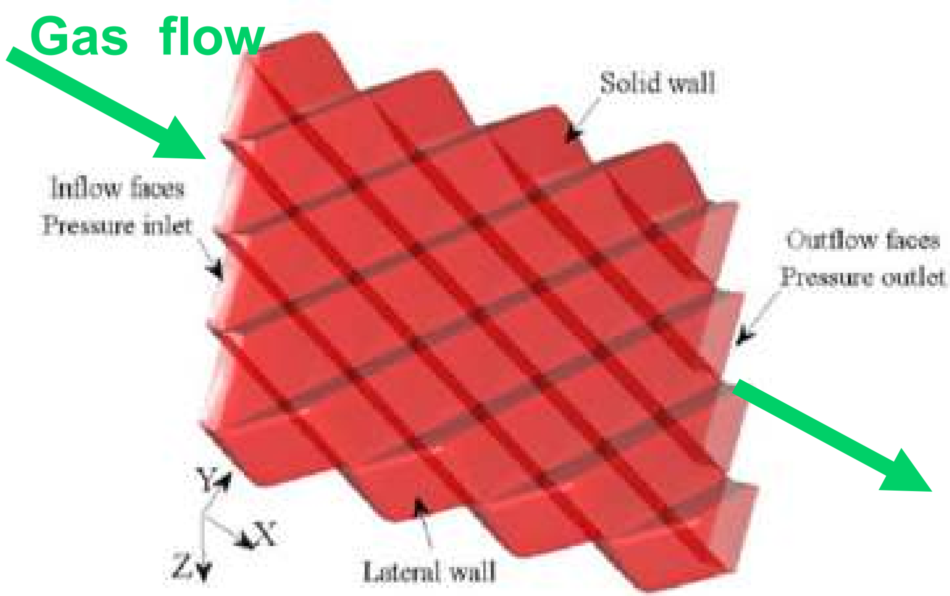

Details

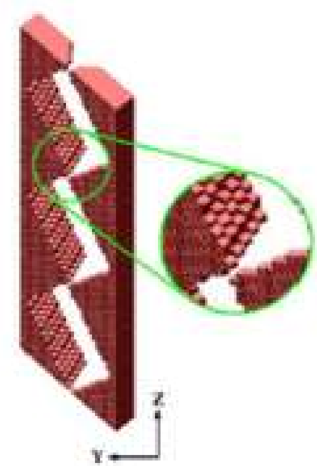

Flow visualization at low Reynolds

- Axial velocity u_X

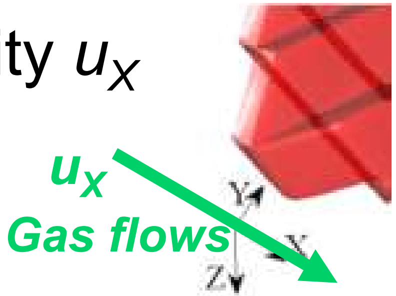

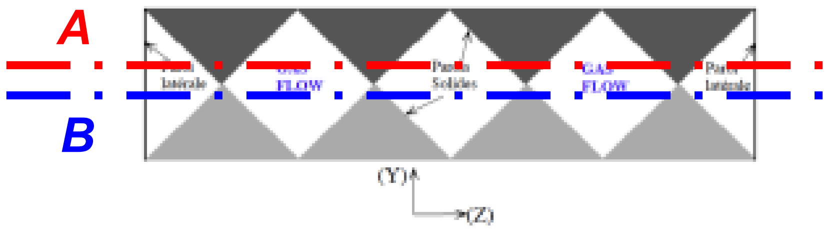

Re = 20 (**SRT-LBE**)

Plane A

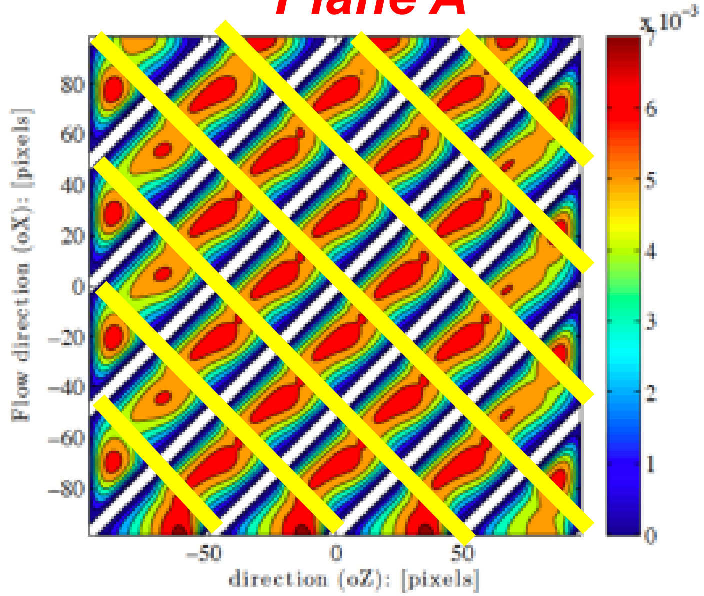

Plane B

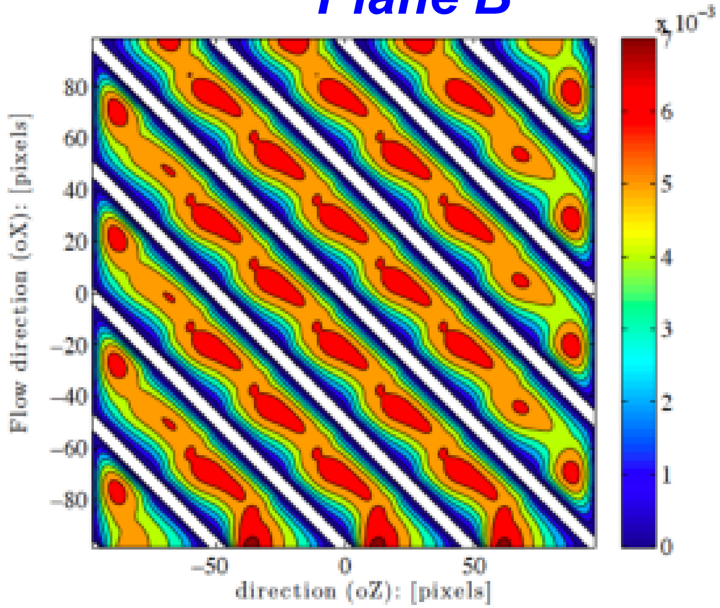

Université de Liège

LGC CHEMICAL ENGINEERING

Flow visualization

At higher Reynolds numbers : **Re > 100**

Plane A

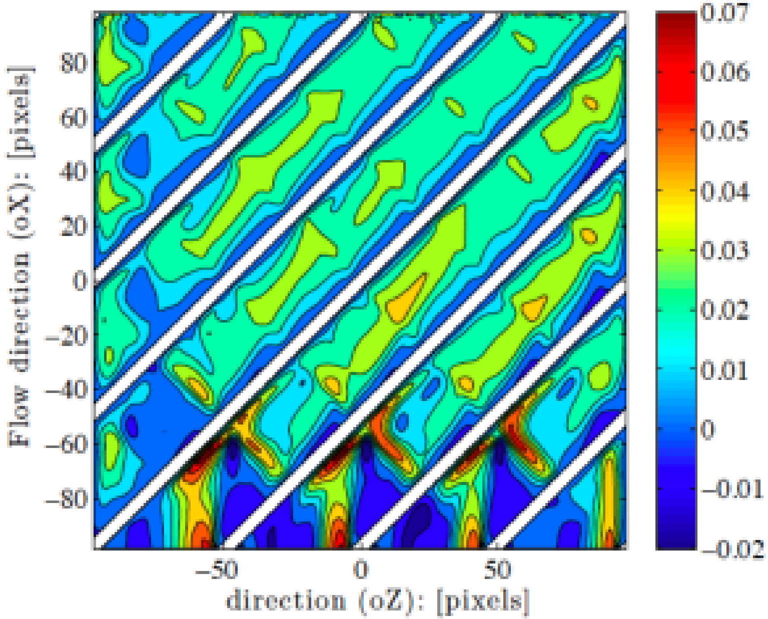

Plane A

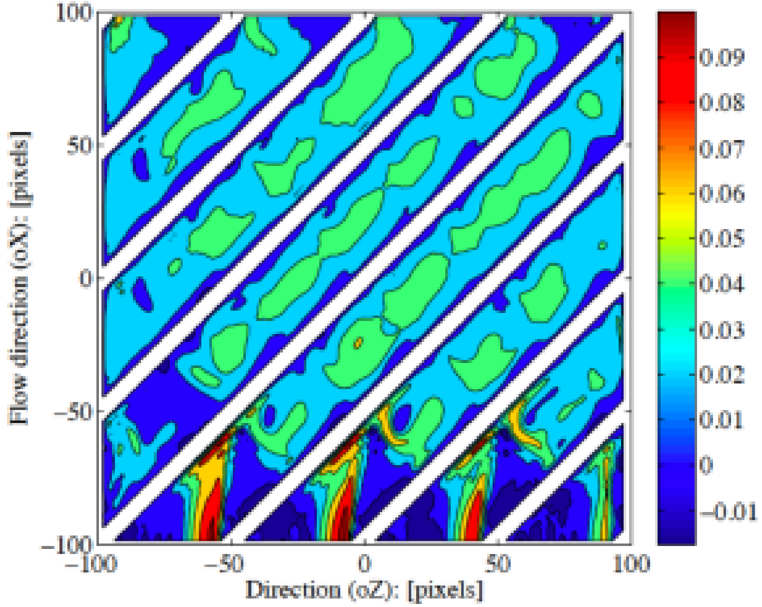

***Re* = 310** **MRT-LBE** ***Re* = 5040**

Pressure drop

$$\frac{\Delta P}{L} = \frac{\rho}{d_P}\frac{(1-\varepsilon)}{\varepsilon^3}\left[A\frac{(1-\varepsilon)}{Re} + B\right]\cdot u_{sup}^2$$

Ergun equation fitted on LB and CFD numerical simulations

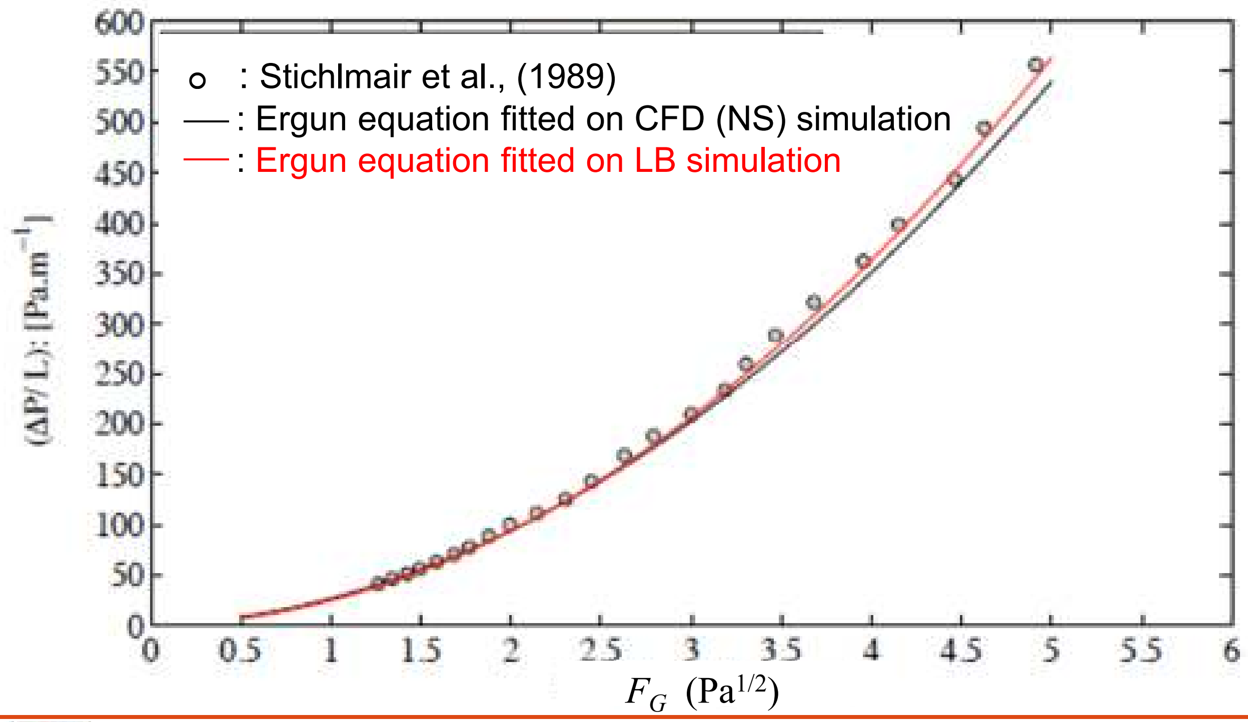

LB sim.	**A = 89**	**B = 0.54**

Stichl. et al.	**A = 80**	**B = 0.37**

Beugre, D., et al.. (2011), Chem. Eng. Sci.

Université de Liège

LGC CHEMICAL ENGINEERING

Two objectives

1. **To get a detailled description of porous media geometry**

   A 3D binary (gas-solid) matrix

   ↳ X-ray (micro)tomographic imaging

2. **To develop a flow simulation model able to deal with the complex geometry of porous media, in terms of boundary conditions**

   A simulation model validated for various complex porous media

   ↳ Lattice Boltzmann method

   A few challenges to take up

CPU and memory requirements

- The numerical resolution of LB equation is simple and straightforward.
- It however requires large execution time and massive memory access
- Two main solutions to reduce these drawbacks:
  - To reduce the sample size: **image undersampling**
  - To **parallelize** the computing architecture

Université de Liège

LGC CHEMICAL ENGINEERING

Image undersampling

- Undersampling consists in sampling a reduced number of voxels from the original image
  - *The sampling rate is defined as the ratio between the total and reduced numbers of voxels, along one direction in the space*

- This modification of the gas-solid interface does not affect significantly the calculated values of pressure drop through an open cell metallic foam (RCM-NCX-1116)

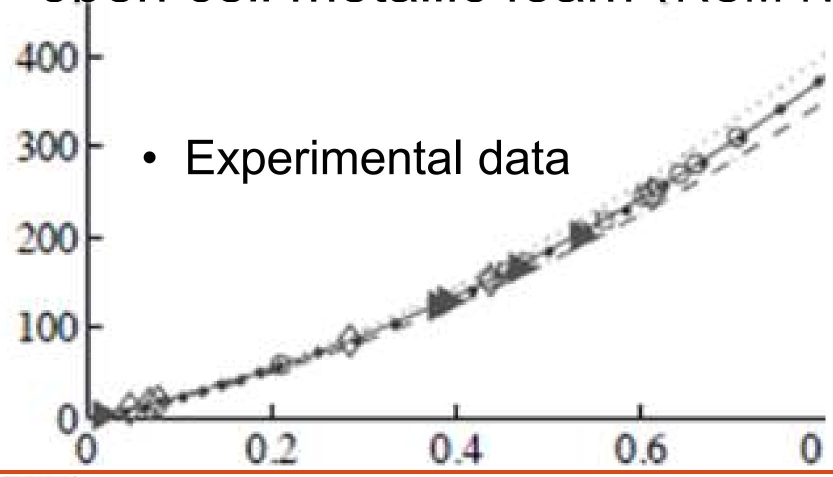

► Sampling rate of 7 voxel size : **224 µm**
◊ Sampling rate of 6
□ Sampling rate of 5
○ Sampling rate of 4
☆ Sampling rate of 3 voxel size : **96 µm**

The pore diameter is around 1.4 mm

Image undersampling

- ***This small modification can probably be explained by the absence of modification of the porous media morphology, e.g., its porosity***

$\times$ **32**

Number of voxels	~ 2 10^5						6.4 10^6
	58^3	67^3	80^3	100^3	134^3	200^3	400^3
Sampling rate	7	6	5	4	3	2	1
Resolution (µm)	224	192	160	128	96	64	32
Porosity (%)	**93.38**	**93.41**	**93.41**	**93.43**	**93.42**	**93.43**	**93.45**

Parallel computing

- An LB simulation can hardly be executed on a single PC:
  - 10 gigabytes of memory and more than 10000 time steps are typically required
  - On a computer with a Pentium IV 3GHz processor, equipped with enough memory, it would take around 2 years to complete the simulation’s execution.
- The LB simulation can easily be executed in a distributed way
  - Using a supercomputer equipped with a great number of identical processors and a large amount of memory
  - Using a cluster of numerous desktop computers interconnected on a grid

Parallel computing

- LB codes are easily adapted to parallelization or task sharing among several computers on a grid

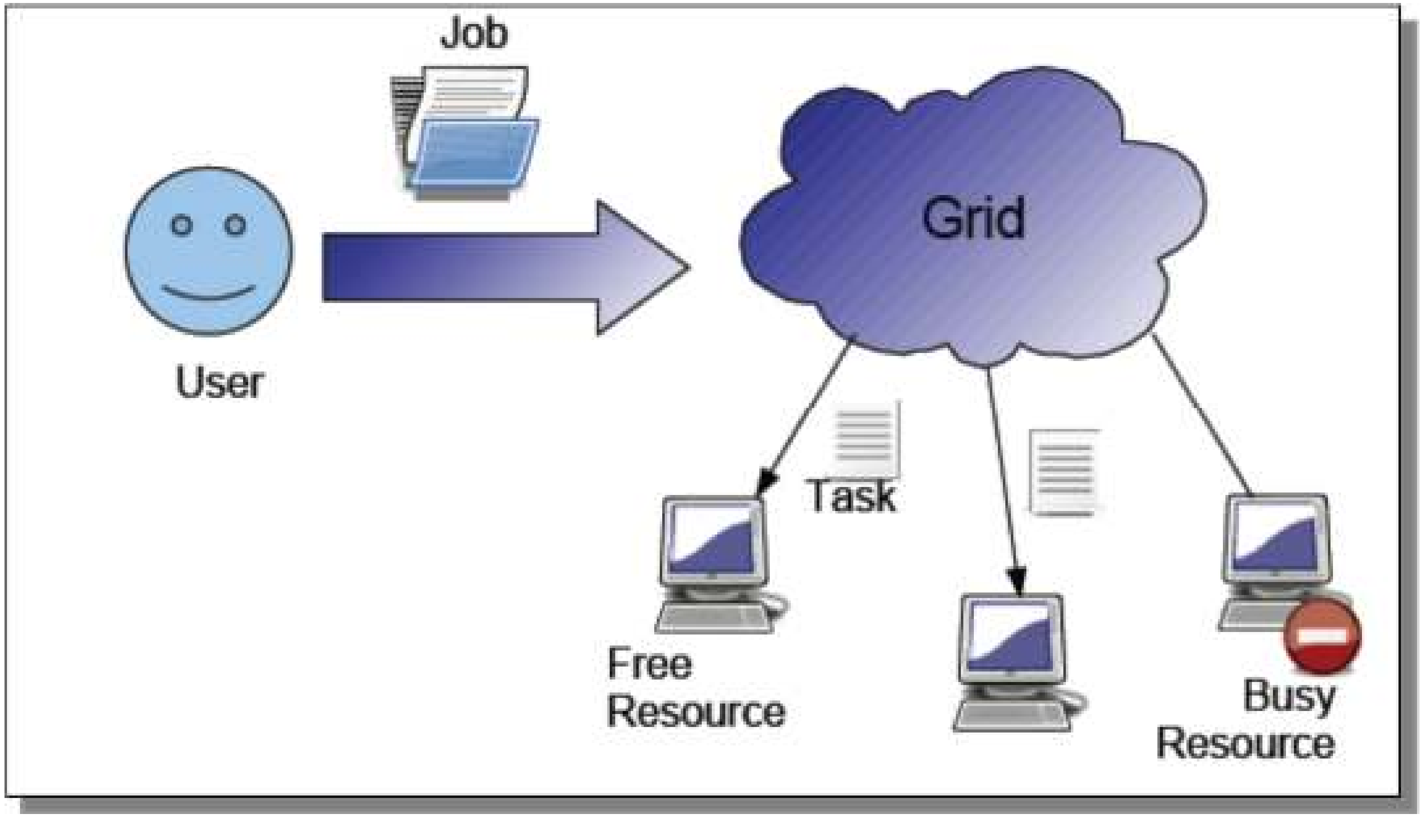

Parallel computing

- Lattice is decomposed into sub-lattices

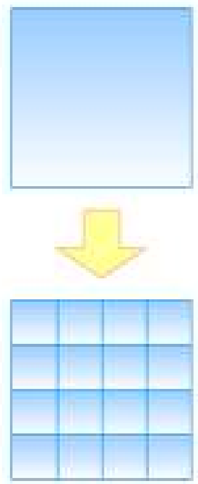

Illustration:

- a 2D lattice decomposed

  into

- 16 sub-lattices

- Sub-lattices can be deployed on different machines

- Data link between sub-lattices

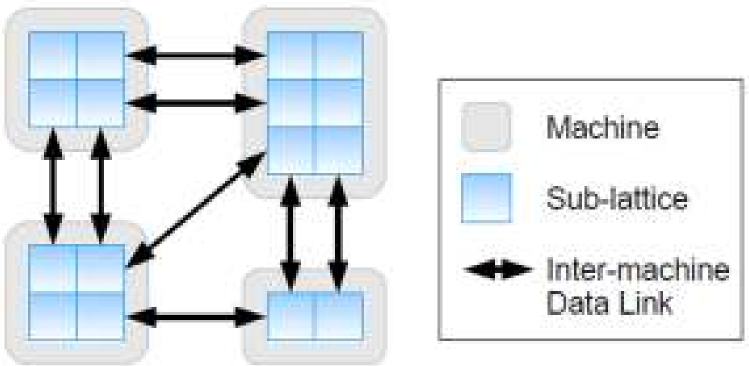

Main challenges

- Distribution on a single (multiprocessors) machine
  - **G1: 2 Xeon dual-core**
    (4 cores), 2.0 Ghz, 4 Mo cache, each with 16 GB of RAM
  - **G2: 6 Xeon dual-core**
    (12 cores), 2.0 Ghz, 4 Mo cache, each with 16 GB of RAM

× 3

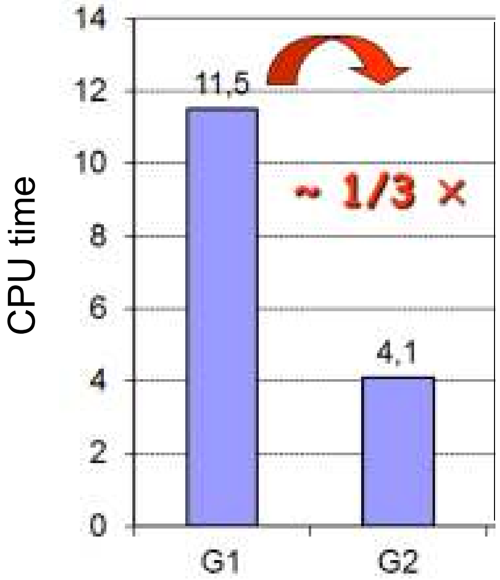

Speedup :

CPU time_1/CPU time_2 = 11,5/4,1 : 2,80

Efficiency :

Speedup/Processor number = 2.8/3 = 0.93 ~ 1

Efficiency almost equal to 1

No time lost in data exchange

Beugre D. et al., 2009, Journal of Computationam & Applied Mathematics

Marchot et a., 2007, ECCE6; Copenhagen

Université de Liège

LGC CHEMICAL ENGINEERING

Main challenges

- Cluster of Pentium Celeron 2.4 Ghz processors inter-connected by a switched-ethernet 100 Mbits network
  - Celeron 2.40 Ghz, 128 ko cache, each with 512 MB of RAM

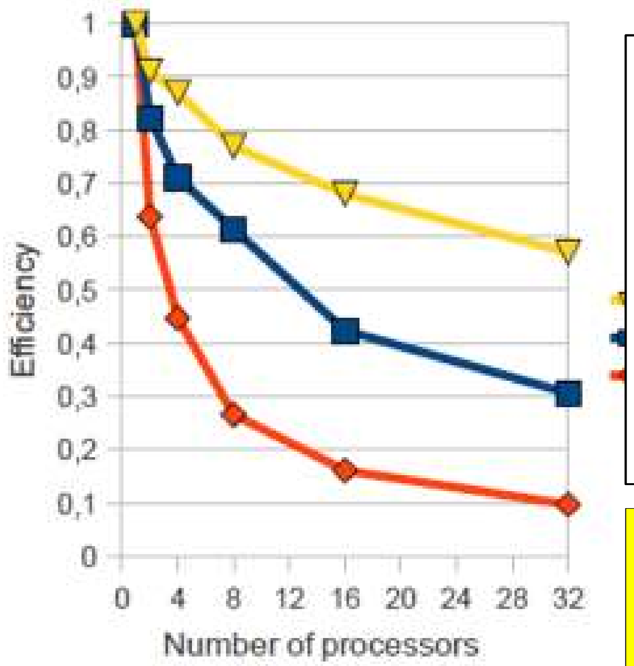

200 times steps on :

- 64-MRT : 64×64×64 sites lattice and a MRT-LB model
- 64-SRT : 64×64×64 sites lattice and a SRT-LB model
- 32-SRT : 32×32×32 sites lattice and a SRT-LB model

Efficiency markedly smaller

Depends on sample size et model complexity

Dethier G.. et al., 2011
Procedia Computer Science

Possible improvements

- Load balancing

  The efficiency of parallel computing in heterogeneous distributed systems (computers of different computational power and memory size), depends strongly on proper load balancing among the computers.

  - *A priori : static load balancing*

    depends on processor parameters, memory available,…

  - *During computation : dynamic load balancing*

    depends …

LaboGrid

a code developed at

LGC

- Computing architecture

  - *Locality :*data associated to addresses that are close in memory address space should be accessed at close moments in time

- Network latency and bandwidth

Two phase flow LB models

- LB models provide are promising tools to describe complex fluid flow in porous media.

- Existing models are based on SRT (BGK) equations applied to the two fluids:

$$\boxed{f_k^{\alpha}\widetilde{(x,t)} = f_k^{\alpha}(x,t) + \Omega_k^{\alpha}(x,t)}$$ Phase α

$$\boxed{f_k^{\beta}\widetilde{(x,t)} = f_k^{\beta}(x,t) + \Omega_k^{\beta}(x,t)}$$ Phase β

- All these models rely on one or several modifications of the BGK collision operator Ω_k

Université de Liège

LGC CHEMICAL ENGINEERING

Two phase flow collision operators

- Introduction of 2 relaxation parameters

$$\Omega_k^{\alpha} = - \frac{1}{\tau\alpha}\left(f_k^{\alpha} - f_k^{\alpha\,(eq)}\right)$$

τ_{α} : relaxation parameter for phase α

$$\Omega_k^{\beta} = - \frac{1}{\tau\beta}\left(f_k^{\beta} - f_k^{\beta\,(eq)}\right)$$

τ_{β} : relaxation parameter for phase β

- Modification of distribution functions at equilibrium to account
- for fluid-solid and fluid-fluid interactions .

- Up to now, surface properties (surface tension and wetting) have been included.

Université de Liège

LGC CHEMICAL ENGINEERING


Thank you for your attention